

NUTRIENT RECOVERY FROM WASTEWATER BY A CONSORTIUM OF ALGAE  
SPECIES FOR BIOFUEL PRODUCTION

by

Edgardo Ayala



A thesis

submitted in partial fulfillment

of the requirements for the degree of

Master of Science in Biology

Boise State University

December 2022

© 2022

Edgardo Ayala

ALL RIGHTS RESERVED

BOISE STATE UNIVERSITY GRADUATE COLLEGE

**DEFENSE COMMITTEE AND FINAL READING APPROVALS**

of the thesis submitted by

Edgardo Ayala

Thesis Title: Nutrient Recovery from Wastewater by a Consortium of Algae Species for Biofuel Production

Date of Final Oral Examination: 30 September 2022

The following individuals read and discussed the thesis submitted by student Edgardo Ayala, and they evaluated the student's presentation and response to questions during the final oral examination. They found that the student passed the final oral examination.

Kevin Feris, Ph.D. Chair, Supervisory Committee

Lisa Warner, Ph.D. Member, Supervisory Committee

Marcelo Serpe, Ph.D. Member, Supervisory Committee

The final reading approval of the thesis was granted by Kevin Feris, Ph.D., Chair of the Supervisory Committee. The thesis was approved by the Graduate College.

## ABSTRACT

Current energy sources are predominantly petroleum-based and their use increases greenhouse gas (GHG) emissions. As the global population grows, and along with it the demand for energy, there is a need to further develop renewable energy sources to avoid the effects of increasing atmospheric CO<sub>2</sub> concentrations on the climate. Biofuels, a renewable energy source, have gained significant interest as a replacement for petroleum-based fuels due to their environmental benefits and carbon neutrality. Biofuels are expected to make up 9.0% of the total fuel consumption in the U.S. by 2040, up from 7.3% in 2019 [1]. Currently, terrestrial crop-based biofuels are the most widely used. However, their production competes for land, fertilizer, and water resources with food production. Cultivation of microalgae-based biofuels can avoid this competition through higher productivity that leads to lower land requirements and their ability to use wastewater as a water and nutrient source for cultivation. We designed and tested a large-scale and semi-continuous operating algal polyculture cultivation system to determine the utility of using undiluted agricultural wastewater as the sole nutrient and water source for algal production. Algal biomass was evaluated for both biofuel production and water treatment (i.e., nutrient sequestration). Algal biomass was converted to a bio-oil by hydrothermal liquefaction (HTL). We also asked if algal production could be maximized by recycling nutrients recovered from HTL processing into a secondary bench-scale algal cultivation system (i.e., in a closed nutrient-loop system). Semi-continuous operations resulted in increased biomass yields, with projections estimated at 4,000 kg biomass/year

in polyhydroxyalkanoate effluent (PHA<sub>E</sub>). Recycling HTL<sub>(aq)</sub> did not present additional benefits in sustaining or increasing algal productivity. Based on our estimations, the highest economic return will result from coupling nitrogen (N) water quality trading (WQT) with biomass conversion to bio-crude.

## TABLE OF CONTENTS

ABSTRACT .....	iv
LIST OF TABLES .....	viii
LIST OF FIGURES .....	ix
LIST OF ABBREVIATIONS.....	xi
CHAPTER ONE: INTRODUCTION.....	1
CHAPTER TWO: MATERIALS AND METHODS .....	8
Growth Conditions and Sampling Scheme for Greenhouse Experiment .....	8
Wastewater Source .....	9
Algal Polyculture.....	10
Growth Monitoring.....	10
Nutrient Analysis.....	11
Carbohydrate and Protein Content .....	11
Lipid Content and Fatty Acid Methyl Ester (FAME) Analysis .....	12
Hydrothermal Liquefaction (HTL).....	12
Growth Conditions and Sampling Scheme for Htl <sub>(Aq)</sub> Amendment Experiment ..	13
Lipid Content and FAME Analysis, HTL <sub>(aq)</sub> Amendment Experiment .....	14
Statistical Analysis, Greenhouse and HTL <sub>(aq)</sub> Amendment Experiments.....	14
CHAPTER THREE: RESULTS.....	16
Greenhouse Experiment.....	16

Biomass Production and Biomass Characterization.....	16
Nutrient Characterization.....	20
HTL Amendment Experiment .....	23
Biomass Characterization .....	23
Nutrient Characterization:.....	26
CHAPTER FOUR: DISCUSSION.....	28
Greenhouse Experiment .....	28
HTL Amendment Experiment .....	32
Annualized Biomass Production Projections: .....	37
Product Yield (Economic Value).....	38
CHAPTER FIVE: CONCLUSION.....	40
REFERENCES.....	54

## LIST OF TABLES

Table 1.	Mean polyculture first order growth rates as determined in the greenhouse cultivation experiment for Chu and PHAE treatments (n=3 per cycle)....	53
Table 2.	Maximum average percent removal and rate of removal of dissolved ammonium, nitrate, and phosphate by the polyculture in Chu and PHAE treatments through three cultivation cycles in the greenhouse experiment (n=3 per cycle).....	53
Table 3.	Fatty acid methyl ester (FAME) average distribution of the polyculture in Chu and PHAE treatments through three greenhouse cultivation cycles (n=3 per cycle).....	53



## LIST OF FIGURES

Figure 1.	Algal biofuel production system with HTL(aq) recycled into upstream cultivation for additional nutrient amendment. Green figures represent biomass cultivation processes. Blue figures represent biomass conversion treatment to generate value added products. Green blue figures represent end products of biomass treatment. Green blue arrow indicates recycling of aqueous phase product back into cultivation experiments. ....	41
Figure 2.	Polyculture growth monitoring via light absorbance (680 nm) in Chu and PHAE treatments throughout three cultivation cycles. Points = mean. Error bars = +/- standard deviation (n=3 for each treatment). ....	42
Figure 3.	Polyculture chlorophyll-a fluorescence in Chu and PHAE treatments through three cultivation cycles. Points = mean. Error bars = +/- standard deviation (n=3 for each treatment). Excitation = 435 nm; Emission = 685 nm. ....	43
Figure 4.	Polyculture cell density (cells/mL) in Chu and PHAE treatments over three cultivation cycles. Points = mean. Error bars = +/- standard deviation (n=3 for each treatment). ....	44
Figure 5.	Polyculture ash free dry weight (AFDW) (g/L) in Chu and PHAE treatments throughout three cultivation cycles. Points = mean. Error bars = +/- standard deviation (n=3 for each treatment). ....	45
Figure 6.	Endpoint measures of carbohydrate, lipid, and protein content for Chu and PHAE treatments in three different rounds of cultivation (mg of analyte/mg of dry biomass). Bars = mean. Error bars = +/- standard deviation (n=3) for each treatment cycle. ....	46
Figure 7.	Dissolved ammonium levels in the PHAE treatment throughout three cultivation cycles (mg/L). Points = mean. Error bars = +/- standard deviation (n=3 for each treatment). ....	47
Figure 8.	Dissolved nitrate levels throughout three cultivation cycles in Chu and PHAE treatments (mg/L). Points = mean. Error bars = +/- standard deviation (n=3 for each treatment). ....	48

Figure 9.	Phosphate levels in Chu and PHAE treatments throughout three cultivation cycles (mg/L). Points = mean. Error bars = +/- standard deviation (n=3 for each treatment).....	49
Figure 10.	Fatty acid profile of the polyculture at the final harvest of cultivation cycles 1(A), 2(B), and 3(C) in Chu and PHAE treatments (mg of lipid/mg of dry biomass). Bars = mean. Error bars = +/- standard deviation (n=3 for each treatment cycle).....	50
Figure 11.	Percent composition of carbohydrate (A), protein (B), and lipid (C) content in dry algal biomass at the end of each cultivation cycle for Chu and PHAE treatments. Bars = mean. Error bars = +/- standard deviation (n=3 for each treatment cycle).....	51
Figure 12.	Chlorophyll efficiency measured by chlorophyll-a fluorescence per unit cell as a function of chlorophyll content in Chu and PHAE treatments. ...	52

## LIST OF ABBREVIATIONS

GHG	Greenhouse Gas
PPM	Parts Per Million
PHA	Polyhydroxyalkanoate
PHAE	Polyhydroxyalkanoate Effluent
AD	Anaerobic Digestion
ADE	Anaerobic Digested Effluent
AFDW	Ash Free Dry Weight
k	First Order Growth Rates
$\text{NH}_4^+$	Dissolved ammonium
$\text{NO}_3^-$	Dissolved nitrate
$\text{PO}_4^{2-}$	Dissolved phosphate
PHAE	Polyhydroxyalkanoate Effluent
HTL	Hydrothermal Liquefaction
$\text{HTL}_{(\text{aq})}$	HTL Aqueous Phase
TN	Total nitrogen
FAME	Fatty Acid Methyl Ester
$A_{680}$	Absorbance
Chl-a	Chlorophyll-a
Chu	Modified Chu 13
MUFAs	Monounsaturated Fatty Acids

PUFA	Polyunsaturated Fatty Acid
GC-MS	Gas Chromatography-Mass Spectrometry
NIST	National Institute of Standards and Technology
WQT	Water Quality Trading
N	nitrogen
P	phosphorus
BGY	Billion Gallons per Year
DOE	Department of Energy
Mmt	Million Metric Tons
HID	High Intensity Discharge
OD	Optical Density
CO <sub>2</sub>	carbon dioxide
CH <sub>3</sub> OH	methanol
H <sub>2</sub> SO <sub>4</sub>	sulfuric Acid
CHCl <sub>3</sub>	chloroform
CH <sub>2</sub> Cl <sub>2</sub>	dichloromethane
U.S.	United States

## CHAPTER ONE: INTRODUCTION

Demand for energy continues to grow globally and is met with increased use of petroleum-based fuels that release significant atmospheric greenhouse gasses [2,3]. Current atmospheric CO<sub>2</sub> levels have reached concentrations of 400 ppm and are expected to increase to 700 ppm in the future, increasing climate temperature by 1.5°C to 2°C [4]. These environmental impacts are highly influenced by anthropogenic activity, primarily by the CO<sub>2</sub> emissions of our petroleum-based transportation industry, which is predicted to remain the highest CO<sub>2</sub> producer through 2050 of any segment of our economy [5]. However, renewable energy sources have gained renewed interest due to their environmental benefits and almost unlimited supply, particularly biofuels [6].

Biofuels are transportation fuels produced from biomass and are considered carbon neutral. They are therefore favored over petroleum fuels from a GHG production perspective [3,7]. These fuels are expected to increase in prevalence in the transportation industry through 2050, peaking close to 9.0% of total fuel consumption in 2040, up from 7.3% in 2019 [1]. In the United States, biofuel consumption has more than doubled from 2000 to 2018 and is projected to increase to a 13.5% share of total fuel composition in the U.S. through 2050 [5]. Increased use of biofuels is expected to be driven by high oil prices, federal and state financial incentives, and policies aimed at energy security and the mitigation of GHG emissions [1,8]. While biofuels have the potential to displace petroleum-based fuels and mitigate climate effects through reduced CO<sub>2</sub> emissions, finding a sustainable production method has been a challenge.

Based on the nature of the feedstocks employed, biofuels are divided into first, second, and third generation biofuels. First generation fuels are known as crop fuels and use various food crops such as corn, sugar cane, soybean, and oil seed to produce bioethanol and biodiesel [9]. Second generation fuels are composed from non-food lignocellulosic material such as forest and crop residues [9]. Third generation fuels are the newest approach and are produced using algae biomass [9]. Currently, crop biofuels are the most viable and commonly used source for biofuels. For example, ethanol sourced from corn products contributes the most biofuel in the United States, 94% of all biofuel produced in 2012 [10]. However, they require considerable amounts of fertilizers and land space that could be allocated towards food production [11,12]. Second-generation fuels alleviate some of these complications by utilizing either non-food crops or non-food components of crops or crop residues [13]. However, second generation fuels have high processing costs that decrease their economic viability [12]. Conversely, algal biofuels (i.e., third generation biofuels) can potentially overcome the high production costs of second generation fuels, require lower resource inputs than first-generation fuels, all while occupying lower amounts of land than first-generation [2,14]. More specifically, microalgae are capable of combining energy capture and fuel production at the cellular level, resulting in efficient fuel production by reducing energy input to non-fermentable plant tissue [15]. In 2007, microalgae were projected to be able to meet 50% of transportation needs in the U.S. using land area between 2 and 4.5 M hectares, which significantly undercuts the 594 to 1540 M hectares needed by terrestrial crop-based fuels to produce the same amount of transportation fuel [16]. While mass production of these

fuels is relatively new, further optimizing algal biofuel production systems is needed before they are produced commercially [3].

Microalgae are single-cell, photosynthetic organisms that can have rapid growth rates and can produce a high energy content per unit of biomass [14]. They have 40-50% higher biomass productivity and photosynthetic efficiency than terrestrial plants [17], a trait that can result in them requiring smaller land area for biofuel production relative to terrestrial plants [18]. For example, microalgae biodiesel productivity is projected at 51,927 (kg/ha/year) while corn and soybean biodiesel productivity is estimated at 152 and 562 (kg/ha/year), respectively [19]. Apart from addressing the challenges of land use and productivity of terrestrial plants, microalgae can also grow using wastewater as a combined source of water and nutrients [18]. Thereby potentially reducing operational and production costs relative to terrestrial crops that require costly nutrient inputs and a fresh water source for cultivation [2,18,20]. As such, microalgae are well adapted for cultivation in municipal and agricultural wastewater since wastewaters are typically enriched in the key macro- and micro-nutrients required for growth of microalgae [21]. Additionally, a variety of algal species can tolerate the osmotic or photochemical parameters typical of municipal and agricultural wastewaters [17,22,23].

Much of the work investigating algae as a biomass source for biofuel production has focused on using individual algal cultivars, or monocultures [24]. However, when grown in outdoor large-scale systems algal monocultures can be prone to invasion by pests, pathogens, or non-target algal competitors [25–27], especially when using wastewater as a nutrient source for growth [23,28]. One way to overcome these challenges is through the utilization of algal polycultures instead of single-species pure

cultures [25–27]. Polycultures are assemblages of distinct algal species that can be naturally occurring or artificially constructed assemblages of algal species [24,29,30]. Research using polycultures has demonstrated that higher levels of productivity are reached as biodiversity increases within a polyculture [31], an outcome known as transgressive over-yielding (i.e., performance of a mixture is higher than expected performance of any single constituent in the mixture) [29,32,33]. This is a trait that is commonly associated with more efficient use of resources [31,33,34]. The specific species combination is important for enhancing productivity [28], while overall species richness tends to be more important for stability, which in turn, can lead to higher net productivity [24,26,27]. In addition to increasing productivity through their community-level interactions, polycultures can resist invasion by grazers and other contaminants that lead to system crashes [24,27]. Therefore, the increase in biodiversity and traits associated with polycultures make them a promising approach to establishing large-scale outdoor algal cultivation systems for biofuel production [27,33]. We explored the use of a naturally occurring polyculture to test its utility in a large-scale wastewater-based cultivation system.

Anthropogenic activity produces considerable amounts of industrial, municipal, and agricultural wastewater that requires treatment to reduce eutrophication of water bodies [20,23]. Eutrophication refers to the enrichment of waters with nutrients such as nitrogen and phosphorus that typically result in algal blooms, oxygen depletion, and a decrease in overall health of aquatic ecosystems [35]. Microalgae can treat a variety of wastewaters by assimilating N and P, and by doing so reduce the potential for eutrophication of natural water bodies [36]. For example, removal rates of dissolved



inorganic nitrogen (sum of the major forms of bio-available N) by microalgae from ADE ranged from 3.2 to 11.2 mg/L/day with a removal efficiency range of 34.3 to 98.4% [29], thereby potentially reducing or eliminating the need for exogenous fertilizers in algal cultivation systems [37]. Exogenous fertilizers are considered the greatest operational costs in terrestrial crops and an obstacle in expanding large-scale algal production systems [36]. A recent study quantified nutrient requirements at 3.85 and 0.87 Mmt of N and P, respectively, to produce 167 Mmt of biomass and generate 10 BGY of renewable fuel [38]. The 10 BGY projection is in line with the renewable energy fuel goals of the DOE by 2030 [39]. Wastewater represents a source of essentially free nutrients and water to sustain microalgae cultivation without competing with food production at a high level.

Anaerobic Digestion (AD) and Polyhydroxyalkanoate (PHA) reactors are resource recovery processes that result in effluents rich in nutrients with the potential to be used in algal cultivation (ADE and PHAE, respectively) [40]. Anaerobic digestion (AD) is used by municipal and agricultural resource recovery facilities and consists of reactors with complex microbial communities that break down organic waste under anaerobic conditions, producing biogas and digestate (residual solids and liquids) [41]. For example, dairies can employ AD to reduce their carbon footprint through carbon sequestration and biogas production [42,43]. Similarly, PHAs can be produced by combining fermented manure and bacteria in aerobic reactors [44]. PHAs are carbon compounds produced and stored by microorganisms under nutrient limiting conditions and can be used to produce bio-plastics [45]. While both processes capture energy from dairy waste, prior work with PHAE has indicated a higher capacity to support algal growth and a 4.1% increase in lipid production when compared to cultivation using

similarly diluted ADE [40]. Here we explore the capacity of undiluted PHAE to support algal growth and lipid production as a means for optimizing cultivation systems with PHAE as the sole nutrient and water source.

Two methods are commonly used to convert algal biomass into biofuels, pyrolysis and hydrothermal liquefaction (HTL). HTL is well suited for wet feedstocks thereby eliminating the need for an energy intensive pre-drying step which is required to treat algal biomass by pyrolysis [46,47]. HTL works by treating biomass with hot, pressurized water over a variable time period, breaking down biomass into primarily liquid components that can be refined to gasoline like fuels [48,49]. HTL of algae biomass also produces an aqueous phase with 25 to 40% of the carbon, and over 50% N from the algae feedstock [50]. The abundant N and P nutrients can be recycled into upstream or secondary algal cultivation systems, ideally maximizing the overall biomass productivity of the system [51].

Recycling HTL aqueous phase (HTL<sub>(aq)</sub>) into upstream cultivation systems shows promise in maximizing algal productivity, however further research is required to fully incorporate HTL aqueous phase into a system [52]. This is due to the toxic compounds associated with HTL aqueous phase, often requiring dilution to reduce the effect of growth inhibitors (phenols, cyclic nitrogen, and NH<sub>4</sub><sup>+</sup>) [53,54]. Previous work has shown that at a small-scale, polycultures make HTL<sub>(aq)</sub> recycling feasible by outperforming monocultures and demonstrating increased productivity [32]. These results were attributed to the polyculture's higher tolerance to aqueous phase stressors [32]. However, the results only indicate the potential for polycultures to recycle HTL<sub>(aq)</sub> nutrients when diluted with standard growth media. Further research is needed to understand polyculture

potential in recycling HTL<sub>(aq)</sub> nutrients in wastewater cultivation mediums. To our knowledge, there is no current study describing the cultivation capacity of HTL<sub>(aq)</sub> amended wastewaters. (Fig. 1) provides an outline of our algal cultivation system and the proposed role of HTL technology in recycling of HTL<sub>(aq)</sub> nutrients to support additional rounds of algal cultivation.

This study employed a large-scale polyculture cultivation system that utilized PHAE as the sole nutrient and water source for algal production. We further explored the utility of the HTL<sub>(aq)</sub>, generated by processing the algal biomass grown in PHAE, as a means for maximizing productivity of a naturally occurring algal polyculture in wastewater. Our experimental design consisted of two cultivation phases: 1) a large-scale semi-continuous biomass cultivation phase that identified the culturing capabilities of PHAE on a naturally occurring polyculture and 2) a bench-scale nutrient amendment phase that explored the utility of recycling HTL<sub>(aq)</sub> nutrients produced from HTL processed biomass into bio-oil (Fig. 1). We hypothesized that PHAE would have the necessary nutrients to support significant polyculture productivity in an outdoor large-scale cultivation system, relative to standard growth medium. We also hypothesized that the polyculture would be able to tolerate HTL<sub>(aq)</sub> amendments and maintain or increase overall productivity as a function of total nitrogen (TN) amended into the PHAE.

## CHAPTER TWO: MATERIALS AND METHODS

### **Growth Conditions and Sampling Scheme for Greenhouse Experiment**

Large-scale algal cultivation raceways were located in the research greenhouse at Boise State University, Boise, Idaho. Raceways consisted of replicate ( $n = 3/\text{treatment}$ ) 100 liter open-top containers (Rubbermaid stock tanks) with clear acrylamide covers and equipped with temperature control (Top Fin submersible heaters and chillers (Trade Wind Chillers, Inc., Model# DI-35) to maintain a mean temperature = 25-30°C). Raceways were continually agitated by circulating pumps (Hydor, Koralia 1150 gph) at opposing sides of the raceways. Ambient temperature in the greenhouse was maintained by an EnviroSTEP control system (Wadsworth Control Systems, Inc.) to a range between 21.1°C and 35°C to align with the ideal algal productivity temperatures ranges between 20°C and 30°C for several algal species [55]. A sunshade was used to reduce excessive temperature increases from solar irradiation. This control of ambient environmental conditions allowed us to closely match seasonal conditions that would be encountered in an outdoor cultivation system. HID sodium lamps were used to keep a minimum photoactive growth period of 18 hours throughout the whole cultivation period. Modified Chu 13 (Chu) [56] was used as the control media and centrifuged PHAE as the treatment media. Raceway treatments (PHAE vs. control) were randomly distributed to help account for light and temperature variation within the greenhouse. Raceways were filled with appropriate treatment media, inoculated with the polyculture, and allowed to reach stationary growth phase. Samples were collected every 48-hours to monitor growth and

collect samples for additional analysis based on time of cultivation (e.g., direct cell counts, dissolved nutrients, and AFDW measurements). Semi-continuous batch operation was achieved by harvesting half of the volume (50 L) in each of the raceways using a 25kg bowl continuous feed centrifuge at approximately 1700 rpm. Full harvest batch operation consisted in harvesting all the volume (100 L) in each raceway similarly. Remaining algae slurry in the centrifuge bowl was pumped into a 4 L vacuum bottle using a vacuum pump (Millipore). Slurry was further concentrated by centrifugation at 4°C and 10,000 rpms for 10 minutes. Harvested biomass was stored at -80°C and lyophilized for use in downstream analysis.

### **Wastewater Source**

Polyhydroxyalkanoate effluent (PHAE) was provided by our collaborator Dr. Erik Coats (University of Idaho). Dr. Coats' lab operates a pilot-scale polyhydroxyalkanoate reactor (200 gallons) situated at the University of Idaho dairy farm (Moscow, Idaho). PHAE is collected from the reactor, centrifuged on site, and frozen before shipping to Boise State University where it was stored at -20°C until used. PHAE was thawed at 4°C before nutrient analysis or subsequent use in algal cultivation. Nutrient content of each PHAE batch was determined by measuring dissolved Nitrate, Phosphate, and Ammonium (see methods below). PHAE was further prepared for cultivation by centrifugation of thawed effluent using a 25kg bowl continuous feed centrifuge at approximately 1700 rpm to remove remaining small particulate matter. The supernatant was then directly used as the growth medium in our experiments with no additional treatment.

### **Algal Polyculture**

The polyculture of algae we employed was originally isolated from the Boise River, and consists of a mixture of *Scenedesmus*, *Chlorella*, *Selenastrum*, *Synechococcus*, a naviculoid diatom, and *Monoraphidium* species [29]. The culture was maintained in a 500 ml Erlenmeyer flask Photobioreactor and a 40 ml borosilicate culture tube with a 400 ml and 30 ml working volume of Modified Chu 13, respectively [56]. Photobioreactor and culture tubes were maintained at room temperature under full spectrum fluorescent lights on a 16:8 light/dark cycle with bi-weekly refresh intervals. Photobioreactors were aerated using an aerator pump (ECOPLUS ECOair4) to promote mixing and introduce ambient CO<sub>2</sub> through a 0.2µm sterile filter (Airekacell) while culture tubes were vented by loosening the caps on the culture tubes to allow gas exchange. Culture tubes were refreshed in new Chu media using 1 mL inoculum from previous cultures. All transfers and inoculations were performed aseptically inside a biosafety cabinet (ThermoScientific).

### **Growth Monitoring**

Algal growth was monitored using non-destructive spectroscopic methods and direct cell counts using a hemocytometer. Optical density was measured at 680 nm (OD<sub>680</sub>) and Chlorophyll fluorescence was measured with an excitation wavelength of 435 nm and emission wavelength of 685 nm. Measurements were obtained using a Synergy Mx plate reader (Biotek). 100 µL samples were loaded onto 96 well plates, black walled 96 well plates were used for fluorescence. Data was compiled to determine exponential growth rates for each replicate. Ash free dry weight (AFDW) analysis was

done gravimetrically using 5 mL samples ( $n = 3/\text{treatment replicate}$ ). Samples were dried overnight at 145°C and ashed at 525°C.

### **Nutrient Analysis**

All nutrients were analyzed using absorbance-based methods and measured using an Aquamate spectrophotometer (ThermoScientific), except for nitrate measurements which were measured using a Synergy Mx plate reader (Biotek). Dissolved nitrate ( $\text{NO}_3^-$ ) was measured using Nitrate TNTplus, LR kits (HACH) with the following modification. Sample and reagent volumes were reduced by equal ratios for use in a 96 well plate. Dissolved phosphate measurements were analyzed using Test 'N Tube reactive Phosphate tubes (HACH) and nitrogen in the form of ammonium was assessed using Lovibond Vario AM tube tests. Measurements for each nutrient were collected on five different time points based on periods of active or slowing growth to determine rates of nutrient assimilation. All samples were filter sterilized using 0.2  $\mu\text{m}$  syringe tip filters (Millipore) prior to analysis. Samples were diluted as necessary to fit within the detection range of each method.

### **Carbohydrate and Protein Content**

Carbohydrate and protein measurements were performed on 5 mg and 2.5 mg of lyophilized biomass, respectively, at the end of each cultivation cycle in the greenhouse scale experiments and at the end of the  $\text{HTL}_{(\text{aq})}$  amendment experiment. Carbohydrate content was measured using a phenol-sulfuric acid method [57] and protein content was measured using a Pierce™ Modified Lowry Protein Assay Kit. Measurements were obtained using a Synergy Mx plate reader (Biotek).

### **Lipid Content and Fatty Acid Methyl Ester (FAME) Analysis**

Lipid content was measured using lyophilized algal biomass collected at the end of each round of cultivation in the greenhouse experiments. The algal biomass ~50 mg was suspended in  $\text{CHCl}_3$  for 18 hours for the extraction of lipids. The aqueous layer was separated and  $\text{CHCl}_3$  was evaporated in glass test tubes and the lipid yield was recorded gravimetrically. The lipid extracts (~2 mg) were heated in a sealed 5 mL reacti-vial<sup>TM</sup> for 90 min at 90 °C in a mixture of  $\text{CH}_3\text{OH}/\text{H}_2\text{SO}_4/\text{CHCl}_3$  (1.7:0.3:2.0 v/v/v, 2 mL) to convert to their FAME derivatives.  $\text{CHCl}_3$  contained 1-naphthaleneacetic acid as an internal standard (200  $\mu\text{g mL}^{-1}$ ). Water was then added to the cooled vial, and after vigorous shaking, the organic layer was collected and dried over anhydrous sodium sulfate. The FAME compounds were analyzed by gas chromatography-mass spectrometry (GC–MS) using a FOCUS-ISQ (ThermoScientific) system at a temperature gradient of 40°C (1 min) to 250°C at the rate of 5 °C  $\text{min}^{-1}$  equipped with a ZB-5 (30 m x 0.25 mmØ, Phenomenex) capillary column. The eluted compounds were identified with authentic  $\text{C}_{12}$  to  $\text{C}_{24}$  fatty acid standards and by spectral matching with the 2017 NIST mass spectral library.

### **Hydrothermal Liquefaction (HTL)**

HTL conversion was performed using a 75-mL Parr Instruments reactor (Model 4740). Each reaction contained 4 g of lyophilized algal biomass and 40 mL water. The reaction temperatures were between 300 and 330 C, with a residence time of 20-40 minutes. The reactor was then cooled, and the aqueous layer was separated from the algae slurry after centrifuging and the yields were recorded. 5 mL of the aqueous phase was



separated for HPLC and freeze dried to record the solids content. The rest of the aqueous phase was used for our HTL amendment experiments as described below.

### **Growth Conditions and Sampling Scheme for Htl<sub>(Aq)</sub> Amendment Experiment**

Nutrient content of the HTL<sub>(aq)</sub> was determined by measuring dissolved Nitrate, Phosphate, and Ammonium (see methods above). HTL<sub>(aq)</sub> treated Chu and PHAE biomass was combined between the three cycles and diluted using regular PHAE, based on total nitrogen (TN) content, to create a master mix containing 35% additional nitrogen relative to the TN present in regular PHAE. Volume from the master mix was used to create additional treatments of 25% and 15% additional nitrogen. Each treatment was inoculated with the polyculture and 300-milliliters aliquoted into sterile 500 ml Erlenmeyer flasks photobioreactors (n = 3/treatment). Similarly, Chu and PHAE treatment master mixes were created, inoculated with polyculture, and 300-milliliter aliquoted into sterile 500 ml Erlenmeyer flasks photobioreactors (n = 3/treatment). Photobioreactors were set to incubate at room temperature under full spectrum fluorescent lights on a 16:8 light/dark cycle. Photobioreactors were aerated using an aerator pump (ECOPLUS ECOair4) to promote mixing and introduce ambient CO<sub>2</sub> through a 0.2µm sterile filter (Airekacell). A 48-hour sampling scheme was employed to monitor growth and collect samples for additional analysis based on time of cultivation (e.g., direct cell counts, dissolved nutrients, and AFDW measurements) through the first 24 days of cultivation (see methods above). Thereafter, a 96-hour sampling scheme was employed to reduce culture sampling volume loss. Biomass was harvested by centrifugation at 4°C and 10,000 rpms for 10 minutes, stored at -80°C and lyophilized for use in downstream analysis.

### **Lipid Content and FAME Analysis, HTL<sub>(aq)</sub> Amendment Experiment**

Lipid content was measured using harvested algal biomass collected at the end of cultivation. Lyophilized algal biomass (~50mg) was suspended in CH<sub>2</sub>Cl<sub>2</sub> (10 mL) for 18 hours with constant shaking (200 rpms) on a BigBill shaker (Thermolyne), then sonicated for 1 minute for the extraction of lipids. Biomass was centrifuged, supernatant recovered in glass tubes and evaporated to dryness to determine lipid yield gravimetrically. Whole biomass samples (~4 mg) were heated in a sealed 5 mL reacti-vial<sup>TM</sup> for 90 min at 90 °C in a mixture of CH<sub>3</sub>OH/H<sub>2</sub>SO<sub>4</sub>/CHCl<sub>3</sub> (1.7:0.3:2.0 v/v/v, 2 mL) to convert to their FAME derivatives. CHCl<sub>3</sub> contained 1-naphthaleneacetic acid as an internal standard (166 µg mL<sup>-1</sup>). Water was then added to the cooled vial, and after vigorous shaking, the organic layer was collected and dried over anhydrous sodium sulfate. The FAME compounds were analyzed by gas chromatography-mass spectrometry (GC-MS) using a FOCUS-ISQ (ThermoScientific) system at a temperature gradient of 40 °C (1 min) to 250°C at the rate of 5 °C min<sup>-1</sup> equipped with a ZB-5 (30 m x 0.25 mmØ, Phenomenex) capillary column. The eluted compounds were identified with authentic C<sub>12</sub> to C<sub>24</sub> fatty acid standards and by spectral matching with the 2017 NIST mass spectral library.

### **Statistical Analysis, Greenhouse and HTL<sub>(aq)</sub> Amendment Experiments**

R version 1.3.1073 was used for statistical analyses. Repeated measures ANOVAs were used to detect differences in biomass yields, nutrient removal rates, protein, carbohydrate, lipid, and fatty acid content between treatments in the greenhouse and HTL<sub>(aq)</sub> amendment experiments. Student's *t*-tests were used to detect differences in biomass yields, nutrient removal rates, protein, carbohydrate, lipid, and fatty acid content between treatments in both the greenhouse and HTL<sub>(aq)</sub> recycling experiments. Data was

assessed for normality (Shapiro test) and homoscedasticity (Bartlett test), non-parametric tests were used when assumptions were not met. All data was collected from three experimental replicates per treatment and presented as the mean values with standard deviations.

## CHAPTER THREE: RESULTS

### **Greenhouse Experiment**

#### Biomass Production and Biomass Characterization

Biomass accumulation was observed in both treatment groups as indicated by increased light absorbance in all three rounds of cultivation (Fig. 2). The PHAE treatment demonstrated a higher inherent light absorption likely due to the presence of chromophoric organic matter and suspended solids in the effluent prior to inoculation with algae. For example, the background absorbance of the PHAE effluent in the absence of an algal inoculum averaged at  $A_{680} = 0.051, 0.051, 0.045$  for each of the three rounds of cultivation, respectively. Whereas the background absorbance of the control Chu media averaged  $A_{680} = 0.034, 0.035, 0.035$  for each of the three cultivation cycles, respectively. Based on the observed patterns of growth in each treatment, samples for AFDW, cell density, phosphate, nitrate, and ammonium were collected at time points where absorbance had increased significantly or the rate of change in absorbance had slowed significantly, indicating the cultures were in the late exponential growth phase or entering stationary phase, respectively. Samples collected at these time points were measured for nutrient levels and culture biomass productivity in each cycle of raceway operation. The PHAE treatment resided in a lag phase longer than the Chu treatment during the first cultivation cycle (e.g., ~10 days vs. 4 days, respectively). However, in subsequent cycles the apparent lag phase of the PHAE treatment was shorter (e.g., ~2 and

0 days in cycles 2 and 3, respectively). Further, there was no significant decrease in the background absorbance of the PHAE treatment at the beginning of cycle 3 (i.e., at the harvest/re-feed at day 46, Fig. 2). This observation in the PHAE treatment was due to increased suspended solids and chromophoric matter not accounted for in the PHAE treatments filter sterilized average absorbance  $A_{680} = 0.045$ . Conversely, the Chu treatment demonstrated a typical decrease in  $A_{680}$  followed by an increase due to outgrowth of the algal culture.

Chlorophyll-a (*chl-a*) measurements tracked polyculture growth and photosynthetic activity throughout the three cultivation cycles (Fig. 3). Culture densities can be proportional to *chl-a* [32], indicating that *chl-a* fluorescence is a good proxy for growth of the algal polyculture. Correspondingly, an increase in algal biomass was observed in the first two cycles of raceway operation (Fig. 3), confirming the *chl-a* fluorescence measurements of both treatments. Contrary to the  $A_{680}$  measurements, an extended lag phase was not observed in the *chl-a* response in the PHAE treatment during the first cycle. This result indicates culture growth and photosynthetic activity in the PHAE treatment during the apparent lag phase as defined by the  $A_{680}$  measurements. The level of change in *chl-a* overtime was lower in the 3rd cycle of operation, however growth was still observed in both treatments. Both treatments experienced a similar decrease in *chl-a* fluorescence intensity after the semi-harvest/re-feed step on day 46, followed by similar photosynthetic activity throughout cycle 3.

Polyculture density as determined by direct microscopic counts (cells/mL), was measured at five different time points in each cultivation cycle (Fig. 4). Measurement timepoints were selected based on timing of cultivation (e.g., start and end of a

cultivation cycle), and periods of active or slowing growth in each treatment for all three cultivation cycles. Similar cell densities were observed in cultivation cycles one and two for both treatments. The PHAE treatment ended cultivation cycles one and two with a lower mean cell density than the Chu treatment ( $1.28 \times 10^7$  cell/mL vs.  $1.86 \times 10^7$  cells/mL and  $1.21 \times 10^7$  cell/mL vs.  $1.99 \times 10^7$  cells/mL in the PHAE and Chu treatments in cycles 1 and 2, respectively). However, this difference in cell density was only significant between the two treatments in the second cycle ( $p$ -value = 0.005) and not in the first cycle ( $p$ -value = 0.145). Following the semi-harvest/re-feed, culture densities in both treatments were reduced to approximately half of the maximum culture density. Final culture densities in cultivation cycle 3 were not significantly different between PHAE and Chu treatments ( $p$ -value = 0.145,  $1.79 \times 10^7$  cell/mL vs.  $1.42 \times 10^7$  cell/mL, respectively). No significant difference in the endpoint cell densities of the Chu treatment was determined across all three cycles ( $p$ -value = 0.188). Conversely, a difference in the endpoint cell densities was detected in the PHAE treatment ( $p$ -value =  $8.68 \times 10^{-3}$ ). A Tukey test indicated cycle 3 was significantly higher than cycles 1 and 2, whereas cycles 1 and 2 did not differ from one another.

First order growth rates ( $k$ ) determined from cell counts are summarized in (Table 1). The  $k$  values were not different between the Chu and PHAE treatments, except for cycle 2 where a higher  $k$  was observed in the Chu treatment ( $p$ -values = 0.169,  $1.71 \times 10^{-3}$ , 0.080, for cycles 1, 2, and 3). This difference follows the general trend of higher  $k$  values in the Chu treatment in cycle 1 while in cycle 3, PHAE averaged a higher  $k$  value than the Chu treatment. The mean  $k$  values did differ as a function of time (i.e., cultivation cycle). More specifically, across the three cycles, a significantly higher first order growth

rate was detected in cycle 2 of the PHAE treatment ( $p$ -value =  $1.34e-02$ ), relative to the first order growth rates in cycles 1 and 3.

Ash free dry weight (AFDW) measures of biomass produced in the PHAE and Chu treatments consistently increased in all three rounds of cultivation (Fig. 5). The Chu treatment averaged a higher AFDW content than the PHAE treatment at the end of each cultivation. However, this difference in AFDW was not statistically different between the two treatments ( $p$ -values = 0.085, 0.084, and 0.376 for cycles 1, 2, and 3). Similarly, AFDW content for both treatments were not statistically different at the start of each cultivation (e.g.,  $p$ -value = 0.243, 0.297, 0.340 for cycles 1, 2, and 3). The final harvest AFDW content in both the Chu and PHAE treatments differed as a function of time (i.e., cultivation cycle) ( $p$ -value =  $5.9e-03$  and  $4.18e-03$ , respectively). A post-hoc Tukey test identified a significant difference in AFDW content between cycles 1 and 3, where cycle 3 had a higher AFDW content relative to cycle 1. AFDW produced in cycle 2 was similar to cycles 1 and 3 in the Chu treatment. AFDW varied between the three cycles in the PHAE treatment, with cycle 3 producing significantly higher AFDW than cycles 1 and 2 ( $p$ -value =  $4.18e-03$ ).

Biomass quality (i.e., protein, carbohydrate, and lipid content) varied between Chu and PHAE treatments (Fig. 6). A difference in the carbohydrate and protein content of the biomass was observed between the two treatments but no difference was observed for lipid content ( $p$ -values =  $7.87e-04$ ,  $3.73e-07$ , and 0.375 respectively). The PHAE treatment yielded biomass with lower carbohydrate content and higher protein content, relative to biomass from the Chu treatment. This response was consistent over all three cultivation cycles with proportions of carbohydrate, lipid, and protein remaining constant

in both treatments across time. No significant difference in carbohydrate content was observed in both the Chu and PHAE treatments across time (p-value: 0.596 and 0.956, respectively), while protein content differed in the Chu treatment across time (p-value =  $2.64 \times 10^{-2}$  and 0.875, respectively). More specifically, a higher protein content was observed in cycle 2, relative to cycle 3. However, the difference between the two cycles of the Chu treatment was small ( $4.6 \times 10^{-2} \pm 2.48 \times 10^{-2}$  mg protein/mg dry weight). Lipid content also varied across time for both the Chu and PHAE treatments (p-value =  $2.55 \times 10^{-2}$ , and  $3.04 \times 10^{-2}$ , respectively). Both treatments had a significantly higher lipid content in cycle 1, relative to cycle 3.

The fatty acid profile of the polyculture was primarily composed of linoleic (C18:2), linolelaidic (C18:2), oleic (C18:1), and palmitic (C16:0) acids in both treatments (Fig. 10, Table 3). No significant difference in the amount of linoleic, linolelaidic, and palmitic acid was observed between the two treatments (p-values = 0.775, 0.673, and 0.190, respectively). Conversely, Oleic acid and stearic acid were produced in significantly higher amounts in the Chu treatment relative to the PHAE treatment (p-values =  $4.10 \times 10^{-4}$  and  $2.68 \times 10^{-2}$ , respectively). Across time, fatty acid amounts were similar in both treatments, with variations of higher linoleic acid in cycle 1 and lower palmitic acid in cycle 3 of the Chu treatment (Fig. 10, p-value =  $9.16 \times 10^{-3}$  and  $3.42 \times 10^{-3}$ , respectively).

### Nutrient Characterization

Dissolved ammonium ( $\text{NH}_4^+$ ) levels in the PHAE treatment were measured at five time points throughout each cultivation cycle (Fig. 7). The Chu treatment was not measured for dissolved  $\text{NH}_4^+$ , as Chu media does not contain  $\text{NH}_4^+$  as a source of



nitrogen. Complete assimilation of  $\text{NH}_4^+$  was observed during each cultivation cycle, resulting in consistent patterns of  $\text{NH}_4^+$  removal. In all three rounds of cultivation approximately 99% removal of  $\text{NH}_4^+$  was achieved. For example,  $\text{NH}_4^+$  concentrations were 0 mg/L after 10 days (e.g., cycles 1 and 3) and 12 days of cultivation (e.g., cycle 2). The specific percent removal differed between the three cycles (p-value = 2.06e-05), however this difference was small (e.g., differences in the 0.01% range). The maximum  $\text{NH}_4^+$  removal rates varied between cultivation cycles (p-value = 1.11e-06) with cycle 1 having the highest removal rate, followed by cycles 3 and 2 (e.g.,  $k = \text{day}^{-1}$ : -0.65, -0.51, and -0.48 respectively).

Dissolved nitrate ( $\text{NO}_3^-$ ) levels in PHAE and Chu treatments were measured at five time points throughout each cultivation cycle (Fig. 8). Initial  $\text{NO}_3^-$  levels were higher in the PHAE treatment, relative to the Chu treatment. Additionally, percent removal was significantly different between the two treatments (p-value = 4.11e-05) with Chu treatment averaging a higher percent  $\text{NO}_3^-$  removal than the PHAE treatment (e.g., 97.8% and 53.2% respectively). Percent  $\text{NO}_3^-$  removal varied between cycles in the Chu treatment (p-value = 2.73e-02), with cycle 2 having a significantly higher percent removal than cycle 3. Percent  $\text{NO}_3^-$  removal also varied across cycles in the PHAE treatment (p-value = 7.34e-03), with a higher percent removal in cycle 2 relative to cycles 1 and 3. The rate of maximum  $\text{NO}_3^-$  assimilation was significantly different between PHAE and Chu treatments (p-value = 4.11e-05). Chu treatment averaged a higher rate of  $\text{NO}_3^-$  removal than the PHAE treatment (e.g.,  $k$ -value =  $\text{day}^{-1}$ : -0.32 and -0.05 respectively). With  $\text{NO}_3^-$  levels in the Chu treatment dropping to single digit concentrations following 12 days of cultivation (e.g., cycles 1 and 2) and 2 days in cycle

3.  $\text{NO}_3^-$  levels were not reduced below 10mg/L in any of the three cycles for the PHAE treatment with variations in  $\text{NO}_3^-$  at harvest being significant (p-value = 8.15e-03). Cycles 1 and 3 contained higher amounts of  $\text{NO}_3^-$  than cycle 2, which correlates with the observed percent removal results (Table 2).

Dissolved phosphate ( $\text{PO}_4^{2-}$ ) levels in PHAE and Chu treatments were measured at five time points throughout each cultivation cycle (Fig. 9). Dissolved  $\text{PO}_4^{2-}$  levels were depleted to concentrations of 0 mg/L in the Chu treatment while in the PHAE treatment this was only observed in the first cultivation cycle (e.g., PHAE cycles 2 and 3 ended with concentrations of 3mg/L and 2mg/L of dissolved  $\text{PO}_4^{2-}$ , respectively). The semi-harvest/re-feed at day 46 replenished one-half the initial  $\text{PO}_4^{2-}$  concentrations of cycle 2 (3.39 mg/L vs. 6.67 mg/L in cycles 2 and 3, respectively). Percent removal of  $\text{PO}_4^{2-}$  was significantly different between the Chu and PHAE treatments (p-value = 1.23e-03), with the Chu treatment averaging a higher percent removal (e.g., 98.6% and 52.8% removal for the Chu and PHAE treatments, respectively). Percent  $\text{PO}_4^{2-}$  removal was consistent and not significantly different between the two treatments (p-value = 5.09e-02) (Table 2). However, rates of maximum  $\text{PO}_4^{2-}$  removal were significantly different between Chu and PHAE treatment (p-value = 9.63e-06). Chu treatment averaged a higher rate of  $\text{PO}_4^{2-}$  removal than the PHAE treatment (e.g., k-value =  $\text{day}^{-1}$ : -0.24 and -0.07, respectively). Additionally, the maximum rate of  $\text{PO}_4^{2-}$  removal did not significantly vary within treatments across the three cultivation cycles.

## HTL Amendment Experiment

### Biomass Characterization

Biomass accumulation was observed in all treatment groups as indicated by the increase in light absorbance ( $A_{680}$ ) (Fig. 13). Growth in the unamended PHAE treatment surpassed growth in the Chu treatment at day 18 and continued to show increased growth through the end of the experiment. Both Chu and unamended PHAE treatments exhibited a higher growth rate and higher final density than the HTL TN-amended treatments. All three HTL TN-amended treatments were observed to have an extended lag phase (increases in  $Abs_{680}$  were not observed until day 12 of cultivation). Conversely, the unamended PHAE treatment entered a more active growth phase near day 8 of cultivation, 4 days before the 25% and 15% HTL TN-amended treatments. The 35% HTL TN-amended treatment had a longer lag phase, lasting approximately 24 days, 12 days more than the 25% and 15% HTL TN-amended treatments. Additionally, light absorbance of the 35% HTL TN-amended treatment indicated this treatment had the lowest growth rate and was also the least dense culture by day 36. Treatments with 25% and 15% HTL TN-amended treatments exhibited an increased growth rate and ending culture density higher than 35% HTL TN-amended treatment. Within the HTL-amended PHAE treatments, the highest growth rate and final culture density was observed in the 15% HTL TN-amended treatment.

Chlorophyll-a measurements monitored polyculture growth and photosynthetic activity throughout the cultivation period (Fig. 14). Chlorophyll-a was highest in the Chu treatment followed by the PHAE treatment and HTL 15% amended treatment. The Chu treatment had overflow measurements following day 28 that exceeded the instruments

limit of detection. An inverse proportion of Chlorophyll-a content to HTL TN amended concentrations was observed, where the HTL 35% amended treatment, the highest TN concentration, contained the lowest chlorophyll-a content.

Polyculture density as determined by direct microscopic counts (cells/mL), was measured at five different time points during the cultivation (i.e., start, end, and periods of active or slowing growth). Cell densities followed typical trends in the Chu and PHAE treatments through the first 20 days of cultivation (Fig. 15). The extended cultivation time to 44 days, allowed for additional cell density increases in both treatments. The PHAE treatment resulted in the highest cell density ( $4.81 \times 10^7$  cells/mL) followed by densities in the Chu, 15%, 25%, and 35% TN HTL<sub>(aq)</sub>, amended treatments ( $3.03 \times 10^7$ ,  $2.23 \times 10^7$ ,  $1.25 \times 10^7$ ,  $7.05 \times 10^6$  cells/mL, respectively). This variation in cell densities resulted in the unamended PHAE treatment producing a significantly higher cell density than all three HTL<sub>(aq)</sub> amended treatments ( $p$ -value =  $3.70 \times 10^{-4}$ , Fig 15). HTL<sub>(aq)</sub>, amended treatments followed a growth curve with an extended lag growth phase, up to 20 days in the 35% TN HTL<sub>(aq)</sub> amended treatment and 16 days in the 15% HTL<sub>(aq)</sub> amended treatment, a minimum of 8 additional days in this growth phase relative to unamended PHAE.

First order growth rates ( $k$ ) from the HTL<sub>(aq)</sub> amendment experiment were determined from cell counts and are summarized in (Table 4).  $k$  was significantly higher in the unamended PHAE treatment compared than all three HTL<sub>(aq)</sub> amended treatments ( $p$ -value =  $9.34 \times 10^{-4}$ , Table 4). Conversely,  $k$  did not differ between Chu treatment and all three HTL<sub>(aq)</sub> amended treatments. However, the chu treatments  $k$  was high enough in similarity to  $k$  in the PHAE treatment.

AFDW measures indicated an increase in organic matter for all five treatments (Fig. 15). Variations in biomass yields were significant across all treatments at time of harvest (p-value =  $1.51 \times 10^{-7}$ ). Both control groups, Chu and PHAE, resulted in the highest AFDW content followed by the 15% TN HTL<sub>(aq)</sub> amended treatment with variations in AFDW not being significant between them. However, with higher levels of HTL<sub>(aq)</sub> amendment, a decrease in the final AFDW content was observed. 35% TN HTL<sub>(aq)</sub> amended treatment resulted in significantly lower AFDW content than all other treatments, with the exception of the 25% TN HTL<sub>(aq)</sub> treatment.

The ratio of macromolecules measured remained constant between the PHAE HTL<sub>(aq)</sub> amended and unamended treatments (Fig. 19). Carbohydrate and protein content were the prominent macromolecules produced, matching the carbohydrate content (p-value = 0.485), but varying in protein content between treatments (p-value =  $5.48 \times 10^{-3}$ ). The lowest protein content was observed in the Chu treatment while the highest protein content was observed in the PHAE HTL<sub>(aq)</sub> amended and unamended treatments. The lipid content in HTL<sub>(aq)</sub> TN amended treatments was lower than in both control groups (i.e., Chu and unamended PHAE). However, no significant difference in lipid production was detected among all five treatments (p-value =  $7.35 \times 10^{-2}$ ).

The fatty acid profile of the polyculture was primarily composed of linoleic, oleic, and palmitic acids (Fig. 20, Table 6). stearic acid, while abundant in the Chu and PHAE unamended treatments, was detected in lower amounts in PHAE HTL<sub>(aq)</sub> amended treatments. A significant difference in the amounts of linoleic, oleic, palmitic and stearic acids was detected between treatments (p-value =  $9.12 \times 10^{-4}$ ,  $6.48 \times 10^{-5}$ ,  $1.09 \times 10^{-4}$ , and  $5.94 \times 10^{-5}$  respectively). All four fatty acids were present in higher amounts in the Chu

treatment with no difference detected between the PHAE unamended and PHAE HTL<sub>(aq)</sub> amended treatments. behenic, arachidic, lauric, lignoceric, and myristic acids were also detected, but were present in lesser amounts in all treatments (Table 6). oleic acid was the highest acid produced for all treatments.

#### Nutrient Characterization:

Dissolved NO<sub>3</sub><sup>-</sup> varied between control and PHAE HTL<sub>(aq)</sub> amended treatments (Fig. 17). A rapid decrease in available NO<sub>3</sub><sup>-</sup> was observed in the Chu treatment after 10 days of cultivation ( $k = -0.331 \text{ day}^{-1}$ ). A slight decreasing trend of available NO<sub>3</sub><sup>-</sup> was observed from start to end in the PHAE treatment ( $k = -8.57\text{e-}03 \text{ day}^{-1}$ ). PHAE HTL<sub>(aq)</sub> amended treatments started with lower NO<sub>3</sub><sup>-</sup> concentrations and experienced an increase in dissolved NO<sub>3</sub><sup>-</sup> through the first 12 days of cultivation. After this, a slight downward trend was observed in the NO<sub>3</sub><sup>-</sup> levels in the 35%, 25%, and 15% PHAE HTL<sub>(aq)</sub> TN amended treatments ( $k = -3.38\text{e-}03, -1.15\text{e-}02, \text{ and } -6.45\text{e-}03 \text{ day}^{-1}$ , respectively). Variations in NO<sub>3</sub><sup>-</sup> removal rates were significant between treatments ( $p\text{-value} = 4.80\text{e-}12$ ), with a higher rate of NO<sub>3</sub><sup>-</sup> removal in the Chu treatment (Table 5). NO<sub>3</sub><sup>-</sup> removal rates in the Chu treatment were approximately 10<sup>3</sup>- greater than the rates in PHAE unamended and HTL<sub>(aq)</sub> amended treatments. NO<sub>3</sub><sup>-</sup> percent removal also varied between treatments ( $p\text{-value} = 8.84\text{e-}06$ ). Chu treatment had a significantly higher NO<sub>3</sub><sup>-</sup> percent removal relative to PHAE unamended and HTL<sub>(aq)</sub> amended treatments.

Dissolved NH<sub>4</sub><sup>+</sup> levels varied between the PHAE unamended and HTL<sub>(aq)</sub> amended treatments. HTL<sub>(aq)</sub> 35% TN amended treatment contained the highest starting NH<sub>4</sub><sup>+</sup> concentration, followed by unamended PHAE, 15% , and 25% HTL<sub>(aq)</sub> TN amended treatments (Fig. 16). The PHAE unamended treatment demonstrated a

decreasing trend in  $\text{NH}_4^+$  concentration across the entire incubation period. Whereas PHAE HTL<sub>(aq)</sub> amended treatments had an initial increase in  $\text{NH}_4^+$  through the first 4 days of cultivation. This was followed by a trend of decreasing  $\text{NH}_4^+$  concentrations through the end of cultivation. With the exception of the HTL<sub>(aq)</sub> 25% TN amended treatment, which illustrated an extended period of increasing dissolved  $\text{NH}_4^+$  through day 12 before a decreasing  $\text{NH}_4^+$  trend was observed. Maximum removal rates and percent removal of  $\text{NH}_4^+$  were not significantly different between PHAE unamended and PHAE HTL<sub>(aq)</sub> amended treatments (p-value = 0.288 and 0.340, respectively) (Table 5).

Dissolved  $\text{PO}_4^{2-}$  levels followed a decreasing trend in the Chu and PHAE unamended treatments while PHAE HTL<sub>(aq)</sub> amended treatments exhibited an initial increase in  $\text{PO}_4^{2-}$  through the first 4 days of cultivation (Fig. 18).  $\text{PO}_4^{2-}$  was completely removed by the end of cultivation in the Chu treatment while small amounts remained in the PHAE unamended and PHAE HTL<sub>(aq)</sub> amended treatments. Variations in  $\text{PO}_4^{2-}$  maximum removal rates were significant between treatments (p-value = 4.03e-05), with a higher removal rate in the Chu treatment than PHAE unamended and PHAE HTL<sub>(aq)</sub> amended treatments (Table 5).  $\text{PO}_4^{2-}$  percent recovered did not differ between the five treatments (p-value = 0.348).

## CHAPTER FOUR: DISCUSSION

### **Greenhouse Experiment**

The cultivation capacity of PHAE met or exceeded that of the standard cultivation media. Semi-continuous batch operation resulted in higher culture densities and AFDW content in the PHAE treatment vs. a standard batch cultivation control. This indicates that semi-continuous batch operation of pilot-scale algal cultivation systems can increase biomass yield and maximize PHAE utility as an algal cultivation medium.

Shading due to suspended particulate organic matter or the presence of chromophoric dissolved organic matter can limit algal photosynthesis and biomass productivity in wastewater-based cultivation media [58]. To determine if shading was influencing algal growth rates and productivity in our system we measured chlorophyll-a fluorescence per cell, a measure previously identified to assess shading effects in algal cultures [32,59]. *Chl-a* fluorescence per unit cell indicated that shading did not occur in both Chu and PHAE treatments. More specifically, chlorophyll emission per cell was consistently higher throughout the cultivation period, indicating that culture densities did not decrease photosynthetic efficiency by decreasing fluorescence as cell densities increased (Fig. 12). However, a lower fluorescence per unit cell was detected in PHAE treatment, relative to fluorescence in Chu treatment. This was likely a result of correcting fluorescence in the PHAE treatment to compensate for emissions from the PHAE alone, with one exception. At the start of cycles 1 and 2, chlorophyll content was higher in the PHAE treatment, potentially due to an initial acclimation to the new cultivation system.



Algal cultivation systems commonly measure overall productivity as a function of biomass yield (AFDW or cells/ml) at the time of harvest [60,61]. In our experiments biomass yield from the consortium of algae tended to be higher in the Chu treatment, however the difference in yield between treatments ( $7.8e+06$  cells/mL) was only significant in the second cultivation. These trends towards higher biomass yields in the Chu treatment were also supported by our AFDW measurements. However, AFDW in all three harvest times was not significantly different between the two treatments. This indicates that using PHAE as a combined nutrient and water source coupled with semi-continuous operations will result in biomass yields similar to those achieved in a standard growth medium. Therefore, our cultivation system is capable of predictable biomass yields when using Chu and PHAE growth media, as first order growth rates did not consistently differ between them. Mean biomass yields in the PHAE treatment ( $0.38 \text{ g/L} \pm 0.21 \text{ AFDW}$ ) was lower than in previous studies cultivating a polyculture in diluted wastewater [29]. However, biomass yields in PHAE ( $3.08 \text{ g/L biomass}$ ) were similar to those of a mixed culture cultivated in diluted dairy digestate [62]. Our data suggests that semi-continuous operation of the algal cultivation system resulted in continuous exponential growth in each treatment, specifically in undiluted PHAE. Demonstrating that similar first order growth rates are achievable when semi-continuous operations are used. This is further supported by the absence of a lag phase in the Chu treatment and only a 2-day lag phase in the PHAE treatment following the semi-harvest/refeed step (Fig. 4).

The macromolecular composition of algal biomass influences its value in downstream products such as bio-oil [63]. The variation in carbohydrate and protein content of the biomass produced in Chu and PHAE treatments is primarily influenced by the availability of dissolved nitrogen. As nitrogen deprivation can result in an increase in either carbohydrate or lipid production [64], two macromolecules that can result in greater bio-oil yield from algal biomass that is processed by HTL [46]. We observed an increase in the relative carbohydrate content of the algal biomass in the Chu treatment when nitrogen was depleted (Fig. 11). Conversely, nitrogen was not depleted in the PHAE treatment leading to higher protein yields relative to the Chu treatment. Protein yields in the PHAE treatment ( $29.9 \pm 0.85\%$ ) closely matched those of previous work where the same polyculture was cultivated in a different type of diluted wastewater ( $28.6 \pm 0.65\%$  protein mass per unit biomass) [29]. However, mean carbohydrate yields ( $13.7 \pm 0.97\%$ ) were 8% lower relative to carbohydrate yields in the same work [29]. Similarly, lipid yield was about 2-5% lower than previous work using mixed consortiums (mean =  $10.4\% \pm 2.5$  and  $9.5\% \pm 1.8$  lipid yield for Chu and PHAE treatments, respectively) [29,65]. Our results suggest the culture was not nutrient limited, therefore no increase in carbon storage was induced and carbohydrates were produced in favor of lipids. Similar observations have been made in polycultures consisting of *Chlorella* and *Scenedesmus* genera [66]. Our polyculture consists of similar genera (i.e., *Scenedesmus*, *Chlorella*, *Selenastrum*, *Synechococcus*, naviculoid diatom, and *Monoraphidium*), suggesting that the effect of nitrogen/nutrient limitation on biomass composition is culture dependent and algal consortiums primarily composed of *Chlorella* may tend to increase carbohydrate content over lipid content under nitrogen deprivation conditions. However, the lipid

content of the polyculture did vary in both treatments as a function of time. Both treatments in cycle 1 resulted in higher lipid content than cycle 3. Suggesting that harvesting at or after 24 days of cultivation (e.g., cycle 1) will yield higher lipid content than harvesting after 18 days or sooner (e.g., cycle 3). Of the measured fatty acids, linoleic acid (C18:2) will compose the highest fraction of the bio-crude, followed by linolelaidic acid (C18:2) (Fig. 10). This will result in bio-crude with higher polyunsaturated fatty acid (PUFA) content, leading to lower fuel viscosity and complete combustion [67]. Previous studies cultivating algae consortiums in wastewater have also identified linoleic acid as a predominate FAME, along with other PUFAs and monounsaturated fatty acids (MUFAs) [68].

Wastewater treatment through algal cultivation can be accomplished through assimilation of dissolved nutrients (e.g.,  $\text{NO}_3^-$ ,  $\text{NH}_4^+$ , and  $\text{PO}_4^{2-}$ ) into biomass [69]. The polyculture we employed was able to assimilate all three monitored nutrients in the PHAE treatment. Dissolved  $\text{NH}_4^+$  levels were reduced in the PHAE treatment, either through microbial oxidation to  $\text{NO}_3^-$  or direct utilization by the algal culture [65,70,71]. This led to a complete removal of  $\text{NH}_4^+$  in the PHAE treatment while  $\text{NO}_3^-$  concentrations remained relatively constant. This resulted in higher rates of  $\text{NO}_3^-$  removal in the Chu media, relative to rates in the PHAE treatment ( $k = -0.317 \pm 0.112 \text{ day}^{-1}$  and  $-0.053 \pm 0.054 \text{ day}^{-1}$ , respectively). The lack of  $\text{NO}_3^-$  decline was likely driven by resident bacteria either introduced as part of the polyculture or present in the PHAE oxidizing the  $\text{NH}_4^+$  into  $\text{NO}_3^-$  [71]. Thereby replenishing the available  $\text{NO}_3^-$  pool and supporting further algal production. Alternatively, the high *Chlorella* makeup of the polyculture may have preferentially assimilated nitrogen in the form of  $\text{NH}_4^+$ , thereby reducing the amount and

rate of  $\text{NO}_3^-$  assimilation, especially in the initial phase of exponential growth phase [72]. Both scenarios are plausible explanations for the apparent lack of  $\text{NO}_3^-$  assimilation in the PHAE treatment. Similar observations by Passero et al. in diluted PHAE were made, where  $\text{NO}_3^-$  removal was not efficient however increased biomass was still observed [40].  $\text{PO}_4^{2-}$  assimilation similarly varied between the two treatments, where percent removal in the Chu treatment was higher than the PHAE treatment ( $98.6 \pm 2.1\%$  and  $52.8 \pm 39.5\%$ , respectively), a difference of ( $45.8 \pm 38.2\%$ ). This is likely a result of the PHAE's organic matter decomposing and releasing  $\text{PO}_4^{2-}$ , reducing P removal efficiency [40].

### **HTL Amendment Experiment**

The utility of the  $\text{HTL}_{(\text{aq})}$  phase for use in algal cultivation can be measured by its effect on biomass yields (AFDW or cells/mL) when the  $\text{HTL}_{(\text{aq})}$  phase is used as a supplementary source of nutrients for algal production. Our results indicate that a 15%  $\text{HTL}_{(\text{aq})}$  amended treatment will result in similar biomass yield (e.g., AFDW) to unamended PHAE and a standard growth medium (1.40, 1.72, and 2.03 g/L AFDW, respectively). Amending with 25%  $\text{HTL}_{(\text{aq})}$  TN and higher decreased the amount of AFDW produced (between 0.80 and 1.30 g/L AFDW), leading to decreased productivity and lower biomass yields. A similar decreasing trend in biomass was observed in a mixed cultures cultivated in dilutions of  $\text{HTL}_{(\text{aq})}$  with municipal wastewater [73]. Conversely, biomass yields as measured by cell counts indicated no significant difference in biomass yields between the three  $\text{HTL}_{(\text{aq})}$  TN amended treatments. Although higher cell densities were observed in the PHAE control treatment, relative to all three  $\text{HTL}_{(\text{aq})}$  TN amended treatments (mean difference ranging from  $2.59\text{e}+07 \pm 1.18\text{e}+07$  to  $4.11\text{e}+07 \pm 1.63\text{e}+07$  cells/mL). Further, the first order growth rate was significantly higher in the PHAE

treatment relative to the rates of all HTL<sub>(aq)</sub> TN amended treatments. Similar observations have been made in cultures of *C. vulgaris* with HTL<sub>(aq)</sub> dilutions, where growth rates decreased with increased HTL<sub>(aq)</sub> makeup [53]. Our growth rates were lower than those observed by Chen et al., however this is likely due to our study using wastewater and not a standard growth medium [53]. Additionally, our study focused on increasing nitrogen in the treatments with HTL<sub>(aq)</sub> addition instead of replacing nitrogen. For example, the growth rate of our highest HTL<sub>(aq)</sub> amended treatment (35% HTL<sub>(aq)</sub> TN amendment,  $0.080 \pm 0.007 \text{ day}^{-1}$ ) was lower than those observed by Chen et al. in the treatment that resulted in growth with the highest HTL<sub>(aq)</sub> makeup ( $0.159 \pm 0.008 \text{ day}^{-1}$ ). However, both of these treatments resulted in similar percent growth rate decreases, relative to their control treatments,  $46.9\% \pm 13.3$  in our experiment and  $47 \pm 7\%$  in the work by Chen et al. [53].

Protein, carbohydrate, and lipid content was measured to determine the effects of the HTL<sub>(aq)</sub> amendments on biomass composition (Fig. 19). Similar to the unamended greenhouse scale experiments, carbohydrate content did not vary between treatments and carbohydrates were produced at a higher level than lipids (Fig. 21). In addition, carbohydrate yields were higher in the Chu and PHAE treatments in the bench-scale experiment, relative to the greenhouse experiment (e.g., difference of  $7.89 \pm 3.15\%$  and  $2.22 \pm 1.53\%$ , respectively). Protein yield was higher in unamended PHAE treatment of the bench-scale experiment while a lower protein yield was observed in the chu treatment, relative to the greenhouse experiment protein yields (e.g., difference of  $8.99 \pm 5.19\%$  and  $10.57 \pm 3.10\%$ , respectively). These variations follow those observed within each treatment during the greenhouse experiment. Protein content was significantly lower

in the Chu treatment, relative to PHAE unamended and HTL<sub>(aq)</sub> amended treatments. This observation is likely a result of the higher nitrogen content available in the PHAE unamended and HTL<sub>(aq)</sub> amended treatments [64]. Similar to the greenhouse experiments, lipid yields were the lowest concentration macromolecule produced and did not vary between treatments (Fig. 19). This observation further supports that our polyculture preferentially produces carbohydrates over lipids in longer cultivations with an extended stationary growth phase [66].

While no variation in lipid yields existed between treatments, the lipid profile did vary between the Chu and PHAE (unamended and amended) treatments (Fig. 20). Chu treatment produced higher amounts of the measured fatty acids, likely due to the extended stationary growth phase under nutrient stress. The lipid profile also varied between the greenhouse and bench-scale experiments, Oleic, Stearic, and Palmitic acids were significantly higher in the bench-scale Chu treatment, relative to fatty acids in the greenhouse experiment. Conversely, the fatty acids measured in PHAE unamended treatments did not vary between the greenhouse and bench-scale experiments, except for higher Linoleic acid yields in the greenhouse experiment (mean difference =  $26.5 \pm 4.10$  mg/g). This observation in the Chu treatment indicates that variation in the lipid profile can result from extended nutrient stress during the stationary growth phase. While the lipid profile generally remained similar in the PHAE unamended treatment between both experiments. Further, the fatty acid profile of the HTL<sub>(aq)</sub> amended treatments was not significantly affected by the HTL<sub>(aq)</sub> amendment, indicating that bio-oil quality will not be adversely affected. However, the longer incubation likely resulted in higher

composition of MUFAs and saturated fatty acids. This composition benefits bio-oil quality, resulting in more stable and increased fuel combustion [67].

Increasing the nutrient load of wastewater through  $\text{HTL}_{(\text{aq})}$  amendment further challenges the polyculture's water treatment ability and influences the wastewater's cultivation capacity.  $\text{HTL}_{(\text{aq})}$  amended treatments were designed based on the TN content of each treatment, as  $\text{HTL}_{(\text{aq})}$  would be used to amend a nitrogen rich media (e.g., PHAE) and the treatment levels would be monitored through  $\text{NO}_3^-$  and  $\text{NH}_4^+$  measurements.  $\text{NO}_3^-$  maximum removal rates were higher in the Chu treatment, whereas PHAE amended or unamended treatments were lower and similar to each other (Table 5). This lack of variation in maximum removal rates between PHAE amended or unamended treatments indicates that  $\text{HTL}_{(\text{aq})}$  amendment does not adversely affect the rate of assimilation, leading to similar water treatment. This is contrary to previous work utilizing diluted treatments of  $\text{HTL}_{(\text{aq})}$  in deionized water, where lower rates were observed at high dilutions and low dilutions of  $\text{HTL}_{(\text{aq})}$  [74]. However,  $\text{NO}_3^-$  percent removal in the PHAE treatment was lower than the percent removal observed in the PHAE treatment during the greenhouse experiment ( $30.0 \pm 17.4\%$  and  $53.2 \pm 9.18\%$ , respectively). Water chemistry and nitrification through microbial oxidation of ammonium can explain this inconsistency [70]. Even with a longer cultivation, levels of dissolved  $\text{NO}_3^-$  fluctuated and were not completely depleted. Variations in  $\text{NH}_4^+$  at the start of cultivation were consistent with the percent amendments of  $\text{HTL}_{(\text{aq})}$  phase. This was largely due to the higher dissolved  $\text{NH}_4^+$  comprising the  $\text{HTL}_{(\text{aq})}$  phase. Maximum removal rates and percent recovery of  $\text{NH}_4^+$  were similar between  $\text{HTL}_{(\text{aq})}$  amended and unamended PHAE treatments (mean  $k$ -value =  $-0.143 \pm 5.64\text{e-}03$  and % recovered =  $99.7 \pm 8.03\text{e-}02\%$ ). Indicating that the

polyculture removes  $\text{NH}_4^+$  from wastewater (i.e., through preferential use or microbial oxidation) even when high levels of  $\text{NH}_4^+$  are present (e.g., 334 mg/L in the 35%  $\text{HTL}_{(\text{aq})}$  TN amended treatment) [71]. Additionally, percent recovery of  $\text{NH}_4^+$  in the unamended PHAE treatment was comparable to those observed in the greenhouse experiment ( $99.8 \pm 0.21\%$  and  $99.6 \pm 1.08\text{e-}02\%$ , respectively) while the maximum rate of assimilation was higher in the greenhouse experiment, relative to the bench-scale experiment (mean difference  $k = -0.408 \pm 2.20\text{e-}02$ ). Removal of  $\text{NH}_4^+$  in the bench scale experiment matched those of previous work utilizing mixed culture and wastewater diluted  $\text{HTL}_{(\text{aq})}$  [73]. Variations in both the percent recovered and rate of  $\text{PO}_4^{2-}$  assimilation between all treatments were not different in the bench-scale experiment. Similarly, percent  $\text{PO}_4^{2-}$  recovered in the Chu and PHAE treatments remained constant and didn't differ between the bench-scale and greenhouse experiment (difference of  $1.19 \pm 0.70\%$  and  $19.7 \pm 51.1\%$  in Chu and PHAE, respectively). Variations in the rates of  $\text{PO}_4^{2-}$  assimilation in Chu and PHAE treatments were also constant between the flask and greenhouse experiments (Chu,  $k = -0.290 \pm 0.077$  vs.  $-0.238 \pm 0.022$  and PHAE,  $k = -0.057 \pm 0.044$  vs.  $-0.067 \pm 0.013$ , respectively). However, dissolved  $\text{PO}_4^{2-}$  recovered was lower than in previous work by Zhou et al., where recovered phosphorus removal was 95% while in our treatments, removal varied between 69-73.6% [73]. This difference in  $\text{PO}_4^{2-}$  removal was likely influenced by filtering the wastewater prior to cultivation which likely removed organic matter that could release dissolved  $\text{PO}_4^{2-}$  throughout the cultivation [40]. Overall, these observations further support the polyculture's ability to assimilate dissolved nutrients in both small enclosed and large open environments.



### Annualized Biomass Production Projections:

To help us understand how our findings relate to a potential commercial scale operation we estimated annualized biomass yields in our large-scale system using semi-continuous operations and our operational conditions. Similar yields for both PHAE unamended and Chu treatments after 18-24 cultivation days (p-value = 0.20 and 0.65, respectively) suggest that we can reasonably predict annualized yields for both system types and treatments categories (e.g., wastewater vs. defined media). We projected annualized biomass yields based on operating a large volume system (1M L) for 270 days/year under semi-continuous operation, a common size and operational duration used to estimate annualized yields [75]. Based on our findings such a system would produce  $3.92 \times 10^3$  kg biomass/year (1,2), where  $v$  = operational volume and  $h$  = number of harvests. while single-batch operations would produce  $1.60 \times 10^3$  kg biomass/year (3), where,  $v$  = operational volume and  $h$  = number of harvests [76]. This results in a difference of  $2.32 \times 10^3$  kg biomass/year, suggesting that semi-continuous operation can increase biomass yields relative to a series of batch cultivations.

$$\text{specific growth rate } (\mu_x) = \frac{X_t - X_0}{t} \quad (1)$$

$$\text{growth kinetics semicontinuous batch } (X) = (X_0 e^{\mu_x t}) \times v \times h \quad (2)$$

$$\text{growth kinetics single batch } (X) = (X_t - X_0) \times v \times h \quad (3)$$

### Product Yield (Economic Value)

The annualized biomass yields of our semi-continuous system can be economically valued into water quality trading (WQT), bio-crude, and cattle feed commodity markets. WQT credits can be sold, through the capture of P and N, that would otherwise be released to watersheds and nonpoint sources [77]. WQT market value fluctuates and is often set through negotiations between the buyer and seller [78]. The WQT market value can range between \$20/lb and \$100/lb for P while N can range between \$4/lb and \$20/lb [79]. In our large-scale cultivation system under semi-continuous operation, income from dissolved P WQT would range between ~ \$300 – ~\$1,600 annually. Estimates for N WQT account for TN in PHAE and are likely over estimated due to the  $\text{NH}_4^+$  derived N undergoing different pathways of transformation that include more than just algal assimilation (e.g., ammonia microbial oxidation). Thus, a projection using  $\text{NO}_3^-$  derived N is a more representative value for N WQT, resulting in an income range of ~\$180,000 – ~\$880,000 annually.

The inefficient removal of dissolved P and N, characteristic of PHAE, likely results in underestimates of N and P via direct measure of dissolved nutrients. Thus, we provide an estimate using the Redfield ratio to approximate recovered N and P in the algal biomass that is produced by our system (4), where  $R_{\%} =$  redfield nutrient % and  $X_y =$  biomass yield [80]. Recovered P and N in biomass from our large-scale cultivation system under semi-continuous operation is estimated at 50 lb/yr and 300 lb/yr, respectively [75]. This would result in additional projected income for P and N of ~\$900 – ~\$5,000 and ~\$1,000 – ~\$7,000, respectively. This would bring

the total projected income from recovered P to a range of ~\$1,300 – ~\$6,300 and recovered N to ~\$180,000 – ~\$890,000.

$$\text{biomass nutrient composition } (X_n) = X_y \times R_{\%} \quad (4)$$

Economically valued biomass yields into other commodities such as bio-crude and high protein cattle feed further supports the utility of a sustainable large-scale algal cultivation system. Under semi-continuous operation, biomass yields valued for bio-crude (assuming 9% lipids and bio-crude price @ \$0.61/L, WTI) would result in potential profits of \$22,000 (5), where  $X_y$  = biomass yield,  $L_{\%}$  = lipid %, and  $V_l$  = oil value [81]. Alternatively, the annualized biomass production can be substituted for high protein cattle feed resulting in potential income between \$14,000 and \$15,000 (6), where  $X_y$  = biomass yield,  $P_{\%}$  = protein %, and  $V_p$  = protein value [82]. Currently, the potential income would decrease if sold as protein cattle feed, even when sold at the high-end, making bio-crude the favorable option with ~\$8,000 in additional income. The ability to alternate between the bio-crude and high protein cattle feed markets can mitigate economic loss by opting for the highest profit return when one market is lower.

$$\text{oil income potential } (I_o) = X_y \times L_{\%} \times V_l \quad (5)$$

$$\text{protein income potential } (I_p) = X_y \times P_{\%} \times V_p \quad (6)$$

## CHAPTER FIVE: CONCLUSION

Overall, our data suggest that both large and small-scale polyculture cultivation systems can produce significant quantities of algal biomass when employing PHAE as the sole nutrient and water source for cultivation. These results suggest that large-scale batch polyculture cultivation systems can efficiently capture nutrients from PHAE and produce significant quantities of algal biomass that can be tuned to be rich in protein or rich in carbohydrates as a function of incubation time. These results indicate that coupling algal cultivation to an integrated bio-product production system that converts solid wastes from dairy systems to bioplastics can reduce the potential for nutrient pollution from a dairy production system while simultaneously producing an additional value-added product stream (e.g., the algal biomass and nutrient trading credits). The high reproducibility between cycles also suggests that our system can be further up scaled. Conversely, amending such a cultivation system with additional nutrients produced via HTL processing of algal biomass does not enhance overall productivity of the system.

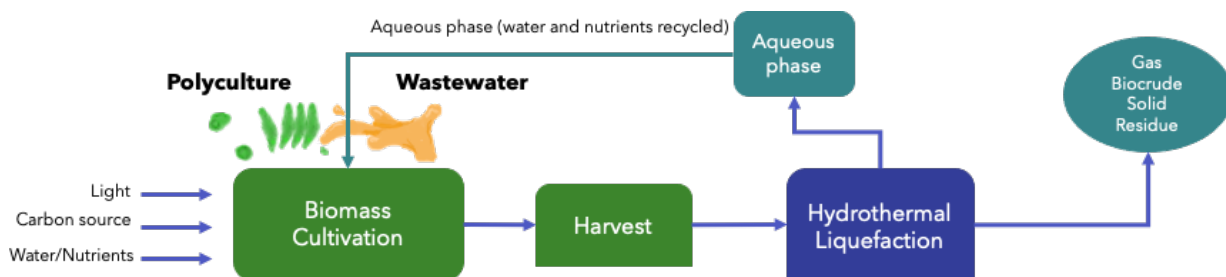


**Figure 1.** Algal biofuel production system with HTL(aq) recycled into upstream cultivation for additional nutrient amendment. Green figures represent biomass cultivation processes. Blue figures represent biomass conversion treatment to generate value added products. Green blue figures represent end products of biomass treatment. Green blue arrow indicates recycling of aqueous phase product back into cultivation experiments.

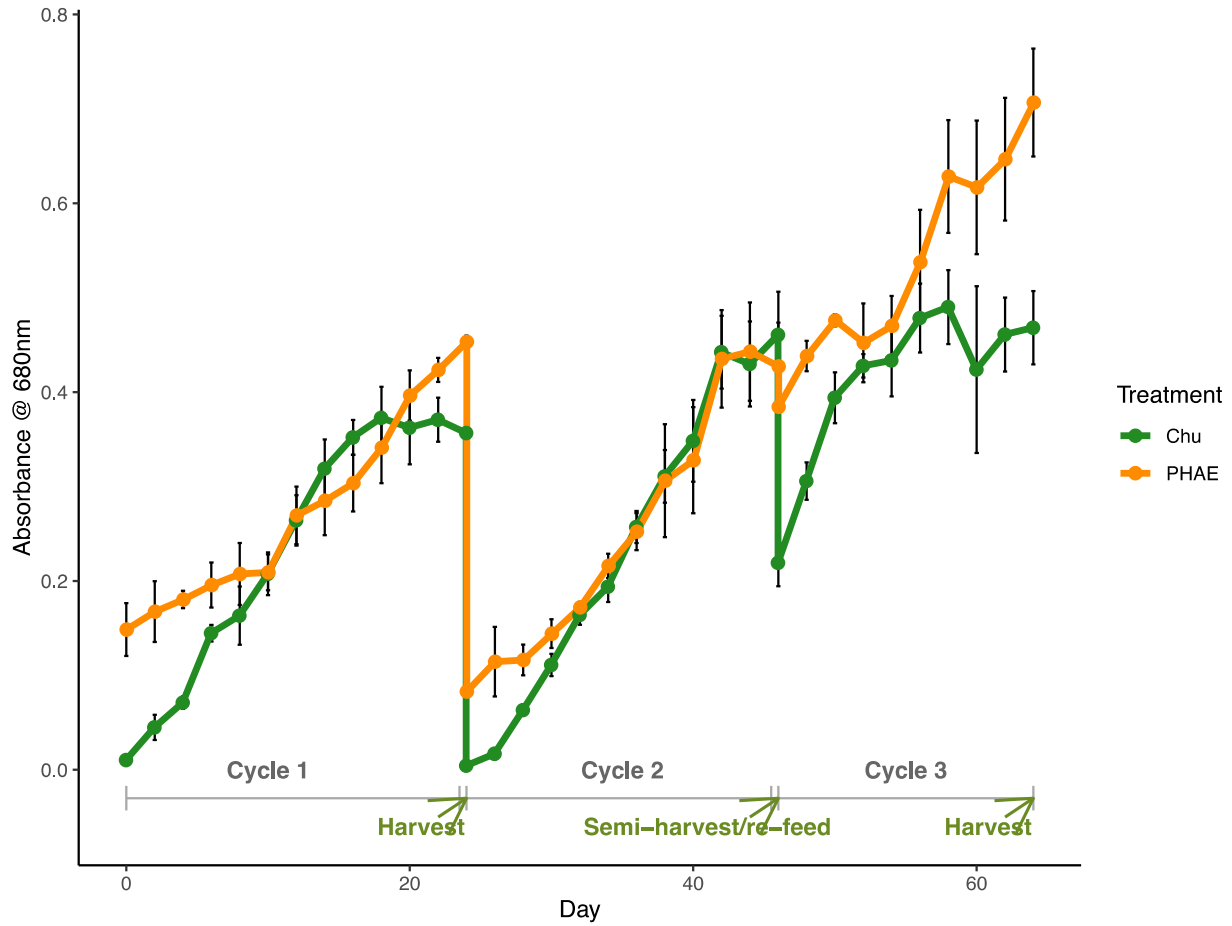


**Figure 2.** Polyculture growth monitoring via light absorbance (680 nm) in Chu and PHAE treatments throughout three cultivation cycles. Points = mean. Error bars = +/- standard deviation (n=3 for each treatment).

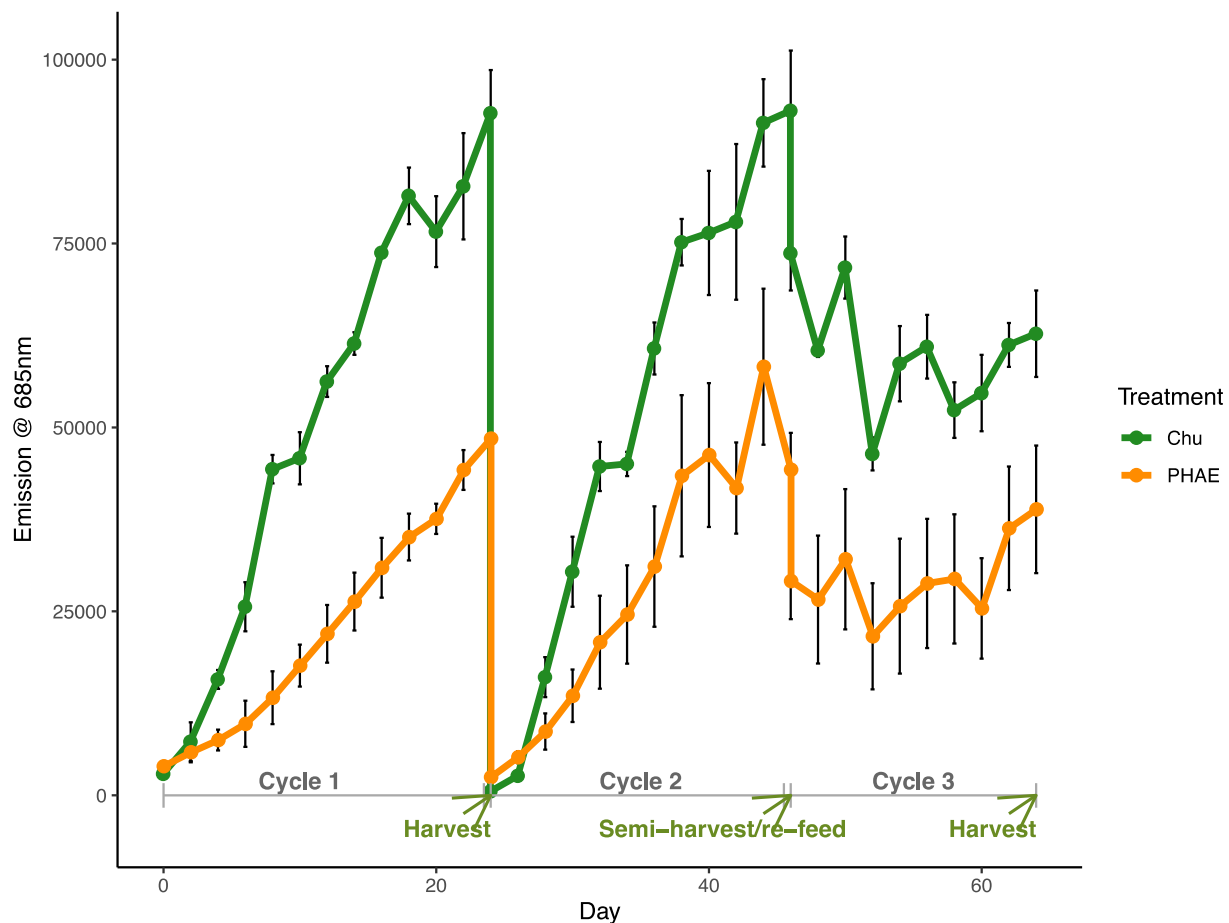


**Figure 3.** Polyculture chlorophyll-a fluorescence in Chu and PHAE treatments through three cultivation cycles. Points = mean. Error bars = +/- standard deviation (n=3 for each treatment). Excitation = 435 nm; Emission = 685 nm.

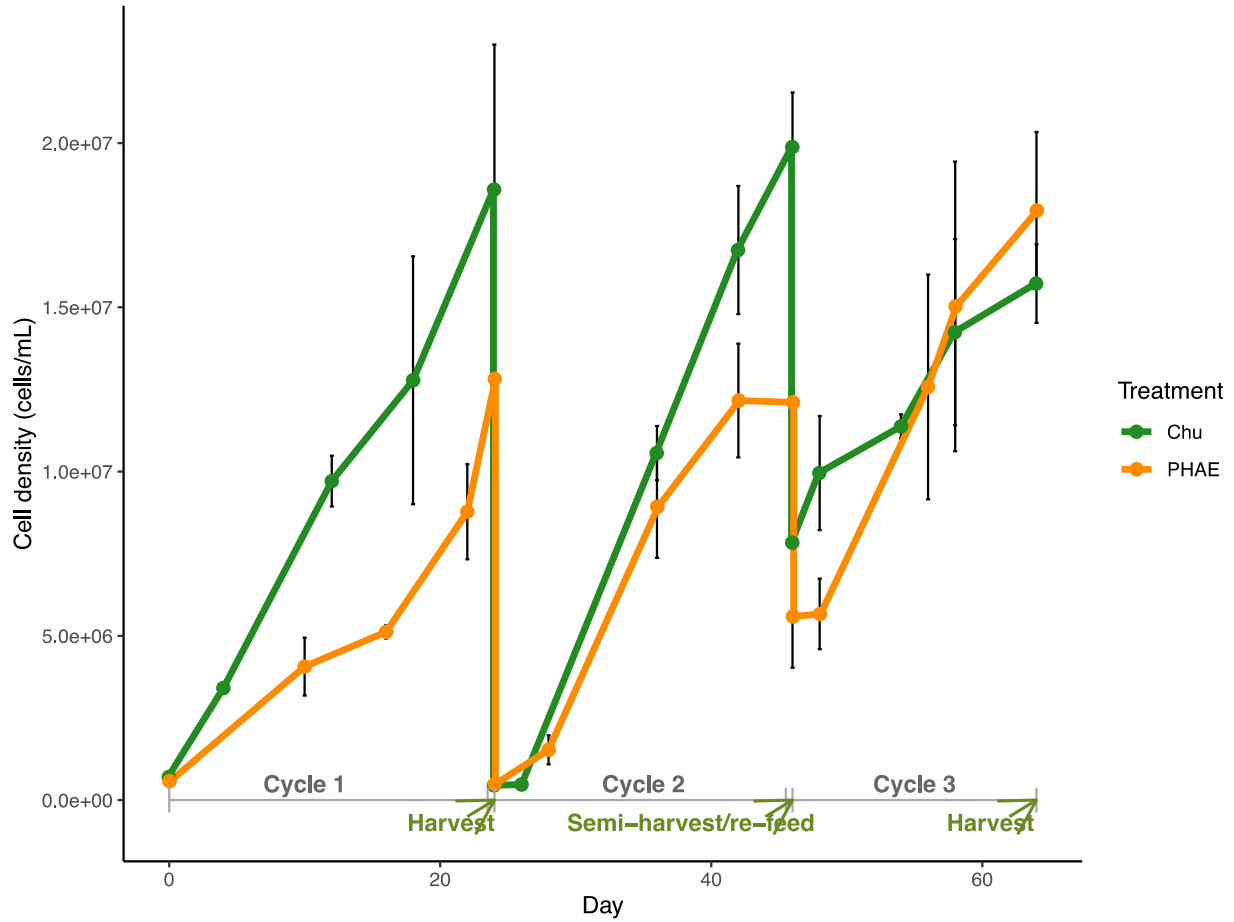


**Figure 4. Polyculture cell density (cells/mL) in Chu and PHAE treatments over three cultivation cycles. Points = mean. Error bars = +/- standard deviation (n=3 for each treatment).**



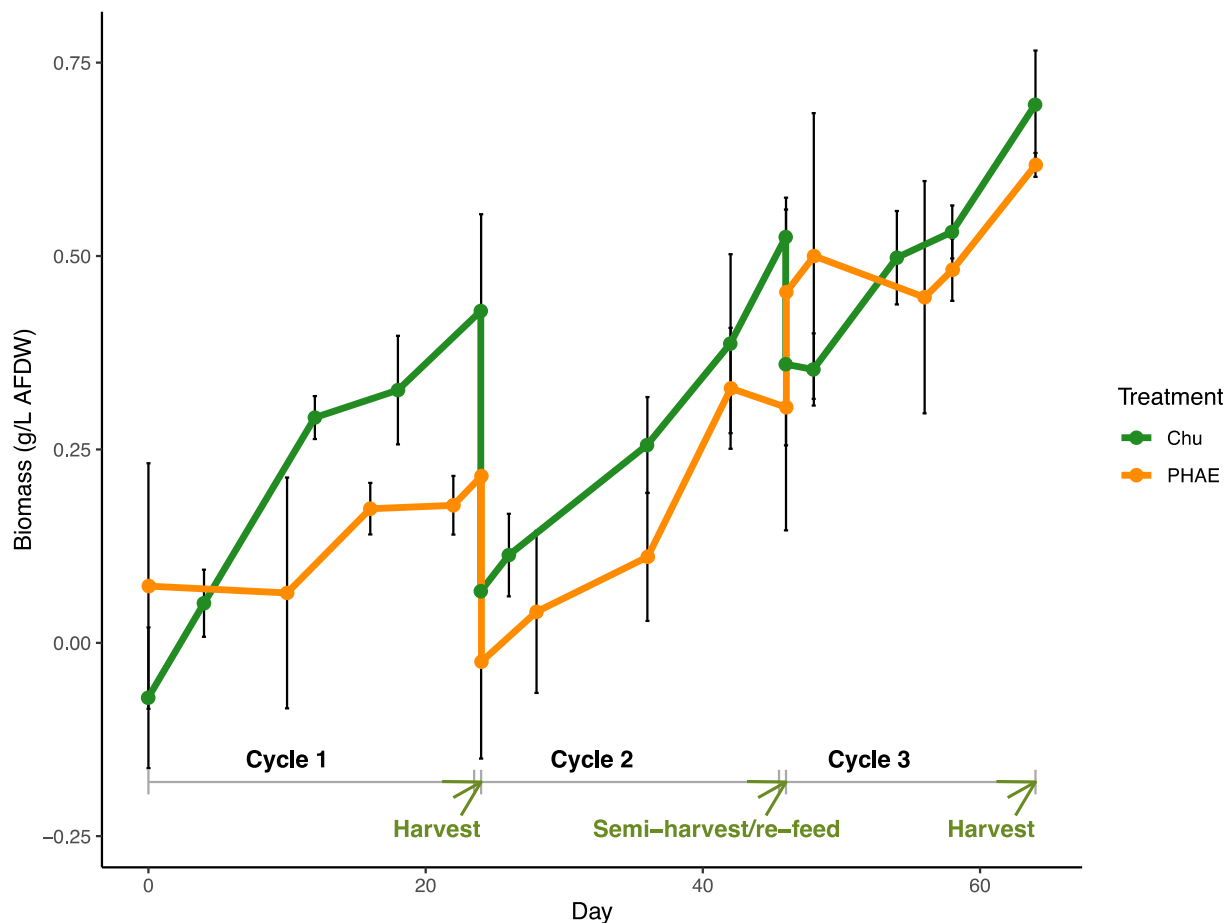


**Figure 5.** Polyculture ash free dry weight (AFDW) (g/L) in Chu and PHAE treatments throughout three cultivation cycles. Points = mean. Error bars = +/- standard deviation (n=3 for each treatment).

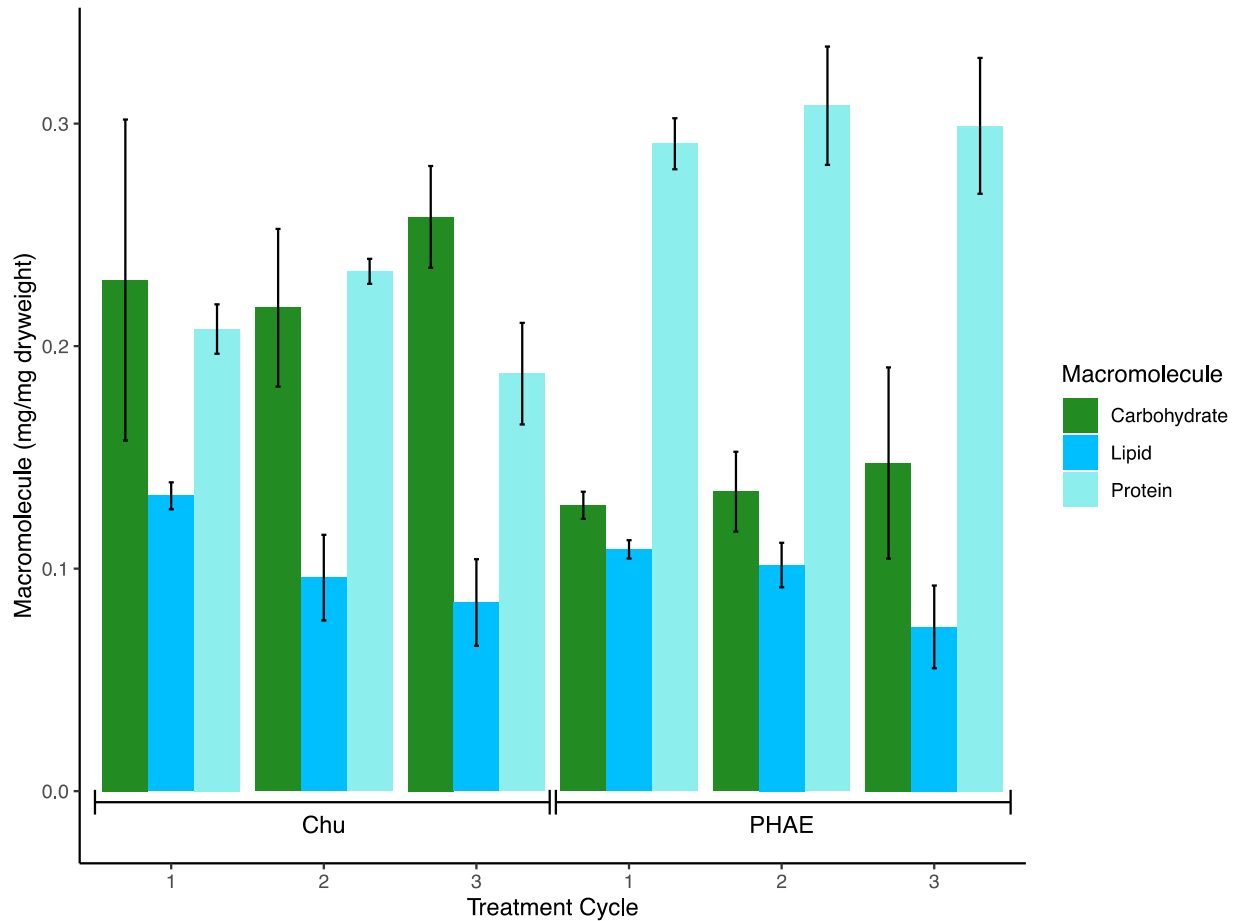


**Figure 6. Endpoint measures of carbohydrate, lipid, and protein content for Chu and PHAE treatments in three different rounds of cultivation (mg of analyte/mg of dry biomass). Bars = mean. Error bars = +/- standard deviation (n=3) for each treatment cycle.**

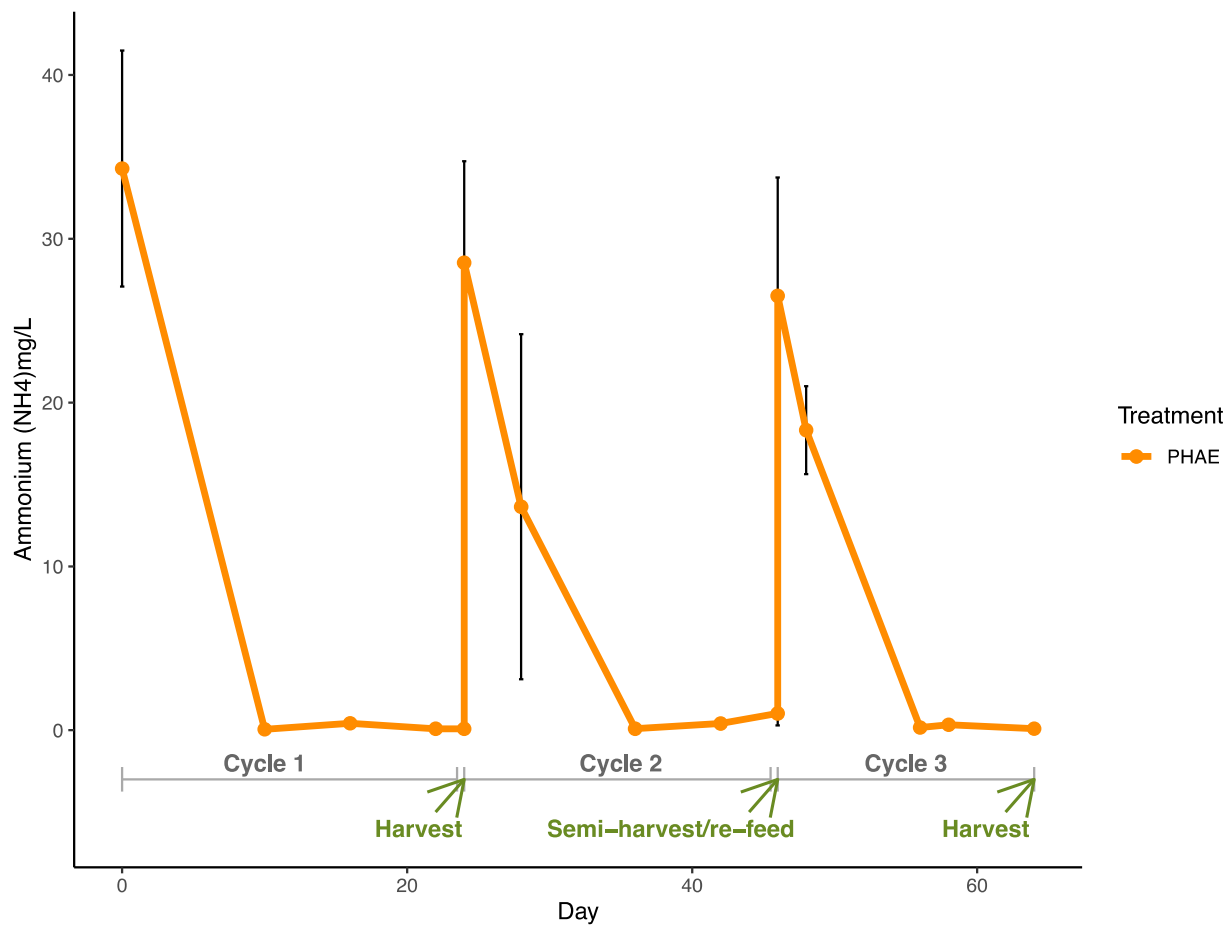


**Figure 7.** Dissolved ammonium levels in the PHAE treatment throughout three cultivation cycles (mg/L). Points = mean. Error bars = +/- standard deviation (n=3 for each treatment).

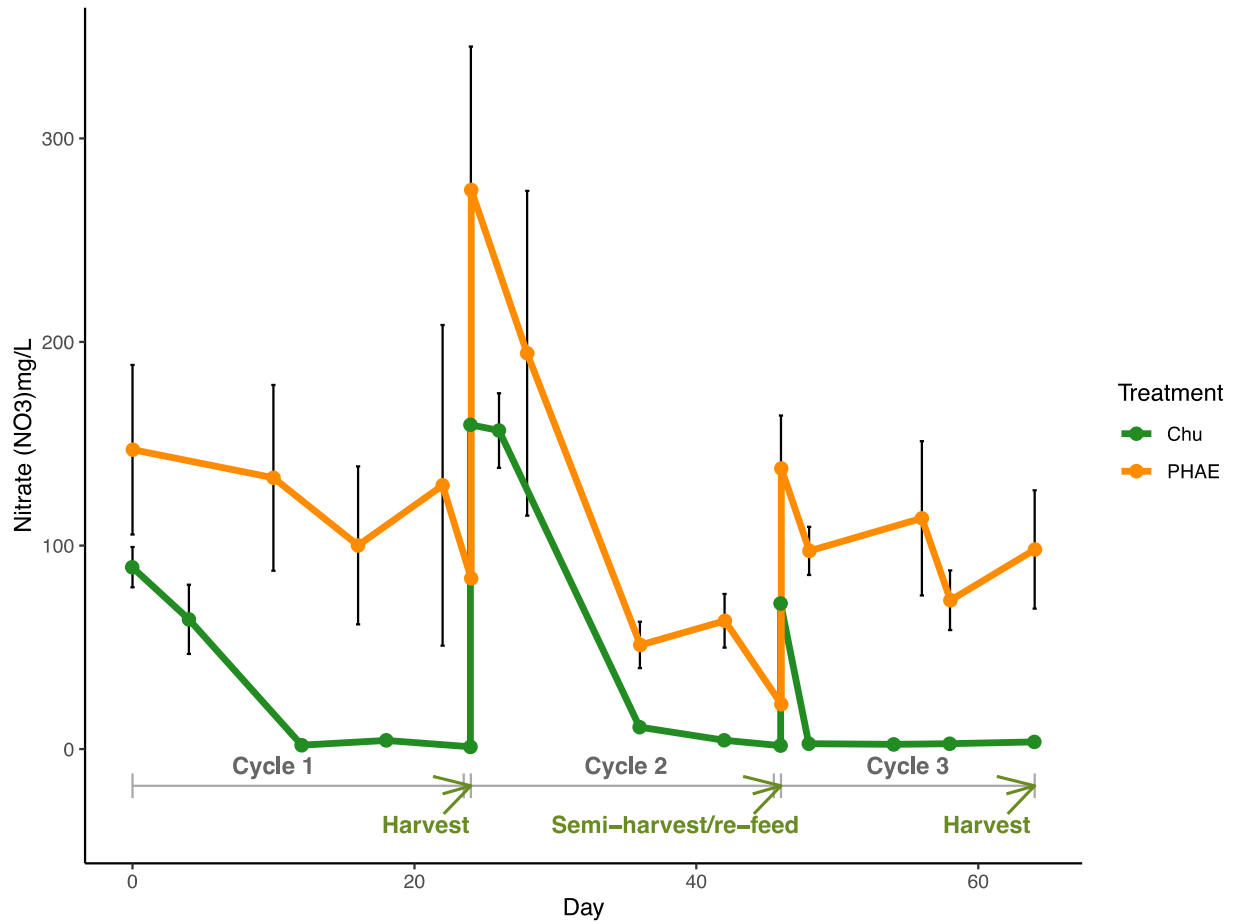


**Figure 8.** Dissolved nitrate levels throughout three cultivation cycles in Chu and PHAE treatments (mg/L). Points = mean. Error bars = +/- standard deviation (n=3 for each treatment).

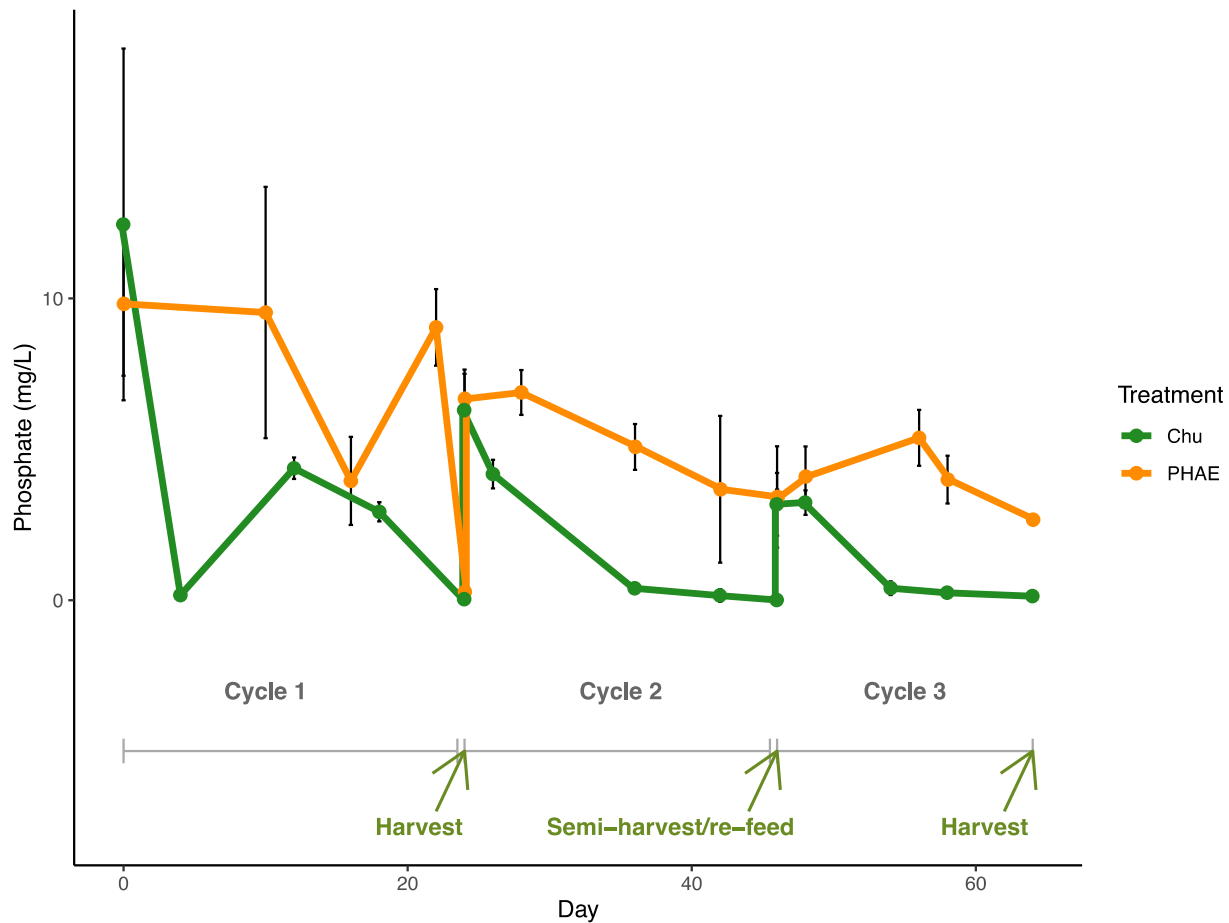


**Figure 9.** Phosphate levels in Chu and PHAE treatments throughout three cultivation cycles (mg/L). Points = mean. Error bars = +/- standard deviation (n=3 for each treatment).

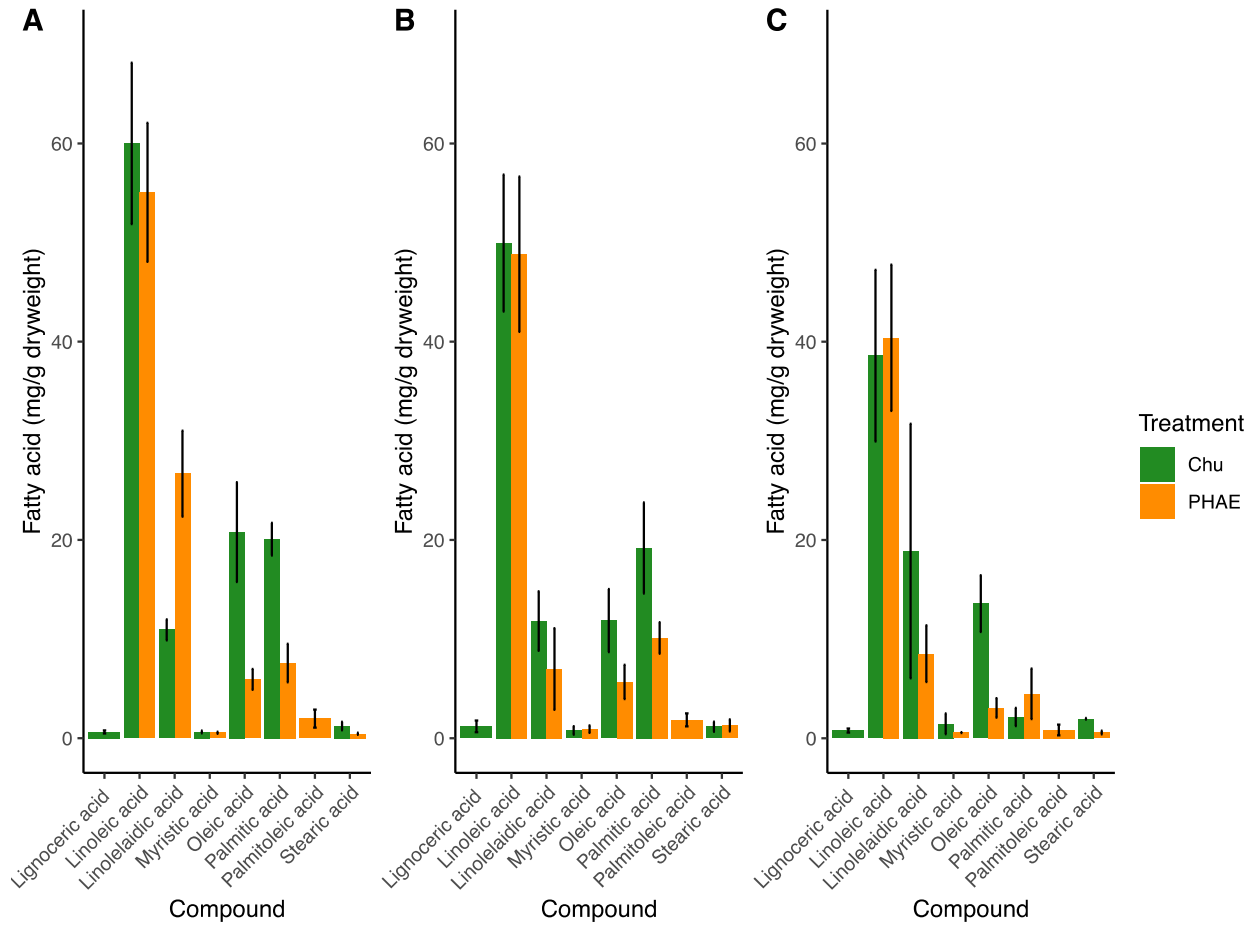


**Figure 10.** Fatty acid profile of the polyculture at the final harvest of cultivation cycles 1(A), 2(B), and 3(C) in Chu and PHAE treatments (mg of lipid/mg of dry biomass). Bars = mean. Error bars = +/- standard deviation (n=3 for each treatment cycle).

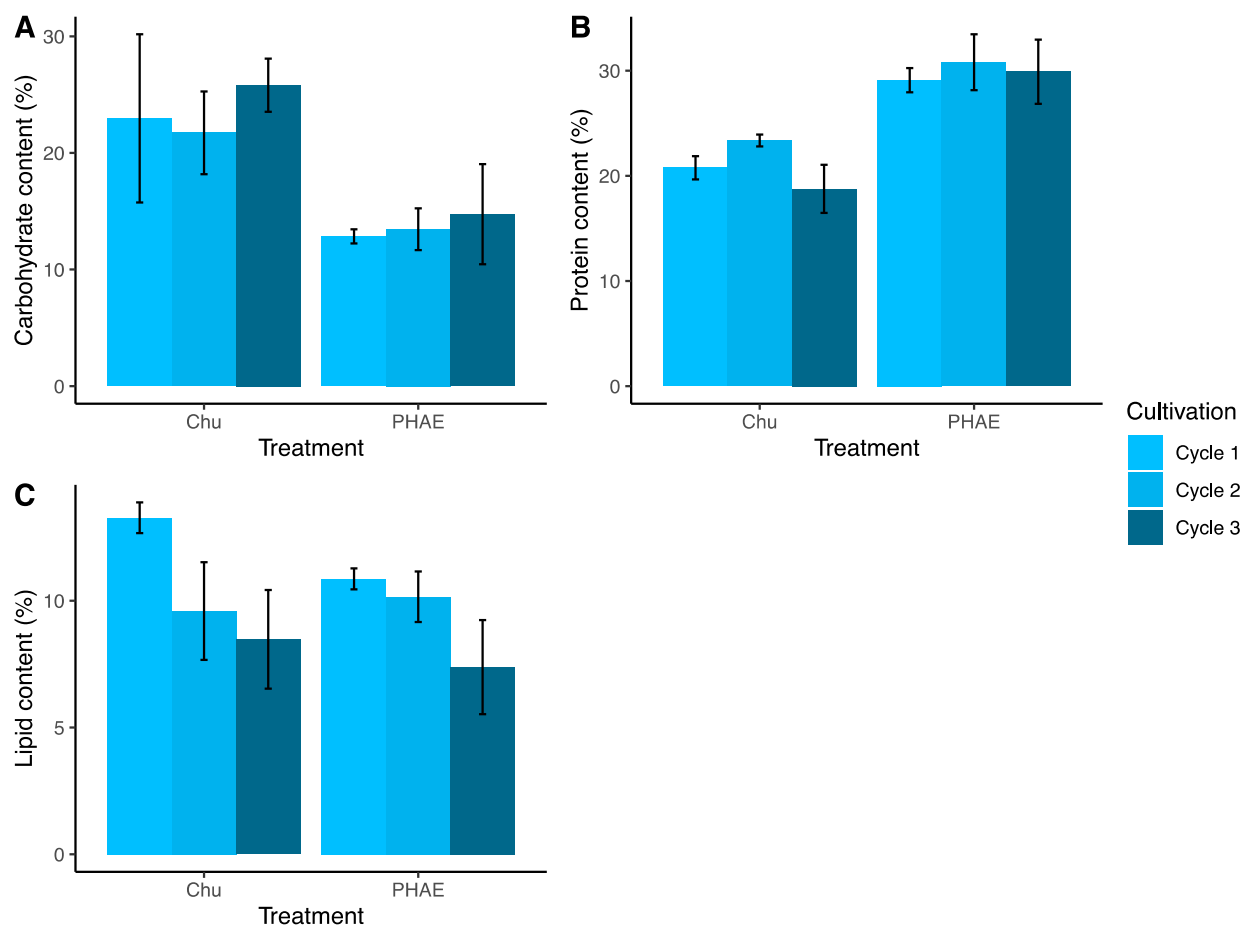


**Figure 11.** Percent composition of carbohydrate (A), protein (B), and lipid (C) content in dry algal biomass at the end of each cultivation cycle for Chu and PHAE treatments. Bars = mean. Error bars = +/- standard deviation (n=3 for each treatment cycle).

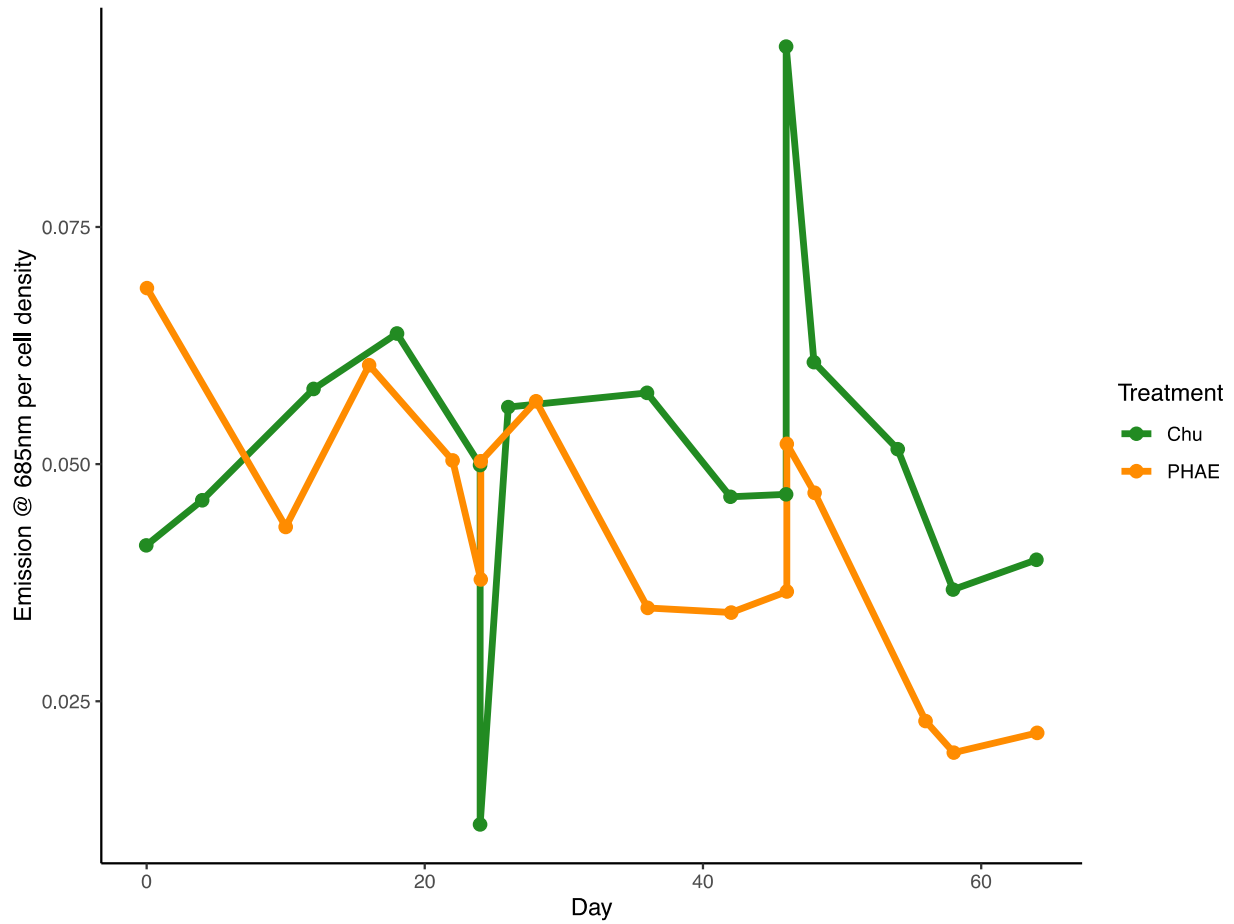


**Figure 12.** Chlorophyll efficiency measured by chlorophyll-a fluorescence per unit cell as a function of chlorophyll content in Chu and PHAE treatments.



**Table 1. Mean polyculture first order growth rates as determined in the greenhouse cultivation experiment for Chu and PHAE treatments (n=3 per cycle).**

Treatment	Cycle	Growth Rate (day <sup>-1</sup> )	
		k	
PHAE	1	0.065	
	2	0.246	
	3	0.096	
Chu	1	0.092	
	2	1.60	
	3	0.036	

**Table 2. Maximum average percent removal and rate of removal of dissolved ammonium, nitrate, and phosphate by the polyculture in Chu and PHAE treatments through three cultivation cycles in the greenhouse experiment (n=3 per cycle).**

Treatment	Cycle	NH <sub>4</sub> <sup>+</sup>		NO <sub>3</sub> <sup>-</sup>		PO <sub>4</sub> <sup>2-</sup>		(n=3)
		% Removal	K	% Removal	K	% Removal	K	
PHAE	1	99.9	-0.654	37.9	-0.023	97.1	-0.149	
	2	99.7	-0.484	92.0	-0.115	40.3	-0.040	
	3	99.4	-0.511	29.7	-0.020	21.1	-0.013	
Chu	1	-	-	97.8	-0.320	99.7	-0.244	
	2	-	-	98.8	-0.204	99.9	-0.267	
	3	-	-	96.7	-0.428	96.2	-0.202	

**Table 3. Fatty acid methyl ester (FAME) average distribution of the polyculture in Chu and PHAE treatments through three greenhouse cultivation cycles (n=3 per cycle).**

Treatment	Cycle	myristic acid	palmitoleic acid	palmitic acid	linolelaidic acid	linoleic acid	oleic acid	stearic acid	lignoceric acid	(n=3)
		C14:0	C16:1	C16:0	C18:2	C18:2	C18:1	C18:0	C24:0	
PHAE	1	0.55	1.98	7.59	26.68	55.07	5.93	0.45	-	
	2	0.92	1.84	10.11	6.98	48.83	5.68	1.29	-	
	3	0.57	0.83	4.48	8.53	40.41	3.06	0.58	-	
Chu	1	0.62	-	20.08	10.93	60.01	20.79	1.22	0.62	
	2	0.78	-	19.19	11.82	49.95	11.86	1.16	1.19	
	3	1.45	-	2.14	18.88	38.60	13.58	1.96	0.77	

## REFERENCES

- [1] Monthly Energy Review – June 2020, (2020) 272.
- [2] J.K. Pittman, A.P. Dean, O. Osundeko, The potential of sustainable algal biofuel production using wastewater resources, *Bioresour Technol.* 102 (2011) 17–25. <https://doi.org/10.1016/j.biortech.2010.06.035>.
- [3] O. US EPA, Economics of Biofuels, (2022). <https://www.epa.gov/environmental-economics/economics-biofuels> (accessed July 18, 2022).
- [4] Summary for Policymakers — Global Warming of 1.5 °C, (n.d.). <https://www.ipcc.ch/sr15/chapter/spm/> (accessed August 28, 2022).
- [5] Annual Energy Outlook 2019 with projections to 2050, (n.d.) 83.
- [6] G. Koçar, N. Civaş, An overview of biofuels from energy crops: Current status and future prospects, *Renewable and Sustainable Energy Reviews.* 28 (2013) 900–916. <https://doi.org/10.1016/j.rser.2013.08.022>.
- [7] Biofuels explained - U.S. Energy Information Administration (EIA), (2022). <https://www.eia.gov/energyexplained/biofuels/> (accessed June 16, 2022).
- [8] World Energy Outlook 2021 – Analysis, IEA. (n.d.). <https://www.iea.org/reports/world-energy-outlook-2021> (accessed August 28, 2022).
- [9] H.A. Alalwan, A.H. Alminshid, H.A.S. Aljaafari, Promising evolution of biofuel generations. Subject review, *Renewable Energy Focus.* 28 (2019) 127–139. <https://doi.org/10.1016/j.ref.2018.12.006>.
- [10] USDA ERS - U.S. Bioenergy Statistics, (2022). <https://www.ers.usda.gov/data-products/u-s-bioenergy-statistics/>.

- [11] W. Thompson, S. Meyer, Second generation biofuels and food crops: Co-products or competitors?, *Global Food Security*. 2 (2013) 89–96.  
<https://doi.org/10.1016/j.gfs.2013.03.001>.
- [12] K. Robak, M. Balcerek, Review of Second Generation Bioethanol Production from Residual Biomass, *Food Technol Biotechnol*. 56 (2018) 174–187.  
<https://doi.org/10.17113/ftb.56.02.18.5428>.
- [13] R.A. Lee, J.-M. Lavoie, From first- to third-generation biofuels: Challenges of producing a commodity from a biomass of increasing complexity, *Animal Frontiers*. 3 (2013) 6–11. <https://doi.org/10.2527/af.2013-0010>.
- [14] M.I. Khan, J.H. Shin, J.D. Kim, The promising future of microalgae: current status, challenges, and optimization of a sustainable and renewable industry for biofuels, feed, and other products, *Microbial Cell Factories*. 17 (2018) 36.  
<https://doi.org/10.1186/s12934-018-0879-x>.
- [15] Y. Liu, P. Cruz-Morales, A. Zargar, M.S. Belcher, B. Pang, E. Englund, Q. Dan, K. Yin, J.D. Keasling, Biofuels for a sustainable future, *Cell*. 184 (2021) 1636–1647. <https://doi.org/10.1016/j.cell.2021.01.052>.
- [16] Y. Chisti, Biodiesel from microalgae, *Biotechnology Advances*. 25 (2007) 294–306. <https://doi.org/10.1016/j.biotechadv.2007.02.001>.
- [17] A. Shahid, S. Malik, H. Zhu, J. Xu, M.Z. Nawaz, S. Nawaz, Md. Asraful Alam, M.A. Mehmood, Cultivating microalgae in wastewater for biomass production, pollutant removal, and atmospheric carbon mitigation; a review, *Science of The Total Environment*. 704 (2020) 135303.  
<https://doi.org/10.1016/j.scitotenv.2019.135303>.
- [18] J. Ullmann, D. Grimm, Algae and their potential for a future bioeconomy, landless food production, and the socio-economic impact of an algae industry, *Org. Agr*. 11 (2021) 261–267. <https://doi.org/10.1007/s13165-020-00337-9>.
- [19] M. Bošnjaković, N. Sinaga, The Perspective of Large-Scale Production of Algae Biodiesel, *Applied Sciences*. 10 (2020) 8181.  
<https://doi.org/10.3390/app10228181>.

- [20] R.K. Goswami, S. Mehariya, P. Verma, R. Lavecchia, A. Zuorro, Microalgae-based biorefineries for sustainable resource recovery from wastewater, *Journal of Water Process Engineering*. 40 (2021) 101747.  
<https://doi.org/10.1016/j.jwpe.2020.101747>.
- [21] S. Jayakumar, M.M. Yusoff, M.H.Ab. Rahim, G.P. Maniam, N. Govindan, The prospect of microalgal biodiesel using agro-industrial and industrial wastes in Malaysia, *Renewable and Sustainable Energy Reviews*. 72 (2017) 33–47.  
<https://doi.org/10.1016/j.rser.2017.01.002>.
- [22] A. Fallahi, N. Hajinajaf, O. Tavakoli, M.H. Sarrafzadeh, Cultivation of Mixed Microalgae Using Municipal Wastewater: Biomass Productivity, Nutrient Removal, and Biochemical Content, *Iran J Biotechnol*. 18 (2020) e2586.  
<https://doi.org/10.30498/IJB.2020.2586>.
- [23] A.L. Gonçalves, J.C.M. Pires, M. Simões, A review on the use of microalgal consortia for wastewater treatment, *Algal Research*. 24 (2017) 403–415.  
<https://doi.org/10.1016/j.algal.2016.11.008>.
- [24] D.T. Newby, T.J. Mathews, R.C. Pate, M.H. Huesemann, T.W. Lane, B.D. Wahlen, S. Mandal, R.K. Engler, K.P. Feris, J.B. Shurin, Assessing the potential of polyculture to accelerate algal biofuel production, *Algal Research*. 19 (2016) 264–277. <https://doi.org/10.1016/j.algal.2016.09.004>.
- [25] Y. Luo, P. Le-Clech, R.K. Henderson, Characterisation of microalgae-based monocultures and mixed cultures for biomass production and wastewater treatment, *Algal Research*. 49 (2020) 101963.  
<https://doi.org/10.1016/j.algal.2020.101963>.
- [26] A.A. Corcoran, W.J. Boeing, Biodiversity Increases the Productivity and Stability of Phytoplankton Communities, *PLOS ONE*. 7 (2012) e49397.  
<https://doi.org/10.1371/journal.pone.0049397>.
- [27] P.K. Thomas, G.P. Dunn, E.R. Coats, D.T. Newby, K.P. Feris, Algal diversity and traits predict biomass yield and grazing resistance in wastewater cultivation, *J Appl Phycol*. 31 (2019) 2323–2334. <https://doi.org/10.1007/s10811-019-01764-2>.

- [28] W. Liu, D. Fu, T. Pan, R.P. Singh, Characterization and Polyculture Analysis of Microalgae Strains Based on Biomass Production and Nutrient Consumption, and Bacterial Community in Municipal Wastewater, *Water*. 13 (2021) 3190. <https://doi.org/10.3390/w13223190>.
- [29] P.K. Thomas, G.P. Dunn, A.R. Good, M.P. Callahan, E.R. Coats, D.T. Newby, K.P. Feris, A natural algal polyculture outperforms an assembled polyculture in wastewater-based open pond biofuel production, *Algal Research*. 40 (2019) 101488. <https://doi.org/10.1016/j.algal.2019.101488>.
- [30] D.E. Berthold, K.G. Shetty, K. Jayachandran, H.D. Laughinghouse, M. Gantar, Enhancing algal biomass and lipid production through bacterial co-culture, *Biomass and Bioenergy*. 122 (2019) 280–289. <https://doi.org/10.1016/j.biombioe.2019.01.033>.
- [31] S. Mandal, J.B. Shurin, R.A. Efroymson, T.J. Mathews, Functional divergence in nitrogen uptake rates explains diversity–productivity relationship in microalgal communities, *Ecosphere*. 9 (2018) e02228. <https://doi.org/10.1002/ecs2.2228>.
- [32] C.M. Godwin, D.C. Hietala, A.R. Lashaway, A. Narwani, P.E. Savage, B.J. Cardinale, Algal polycultures enhance coproduct recycling from hydrothermal liquefaction, *Bioresource Technology*. 224 (2017) 630–638. <https://doi.org/10.1016/j.biortech.2016.11.105>.
- [33] J.B. Shurin, S. Mandal, R.L. Abbott, Trait diversity enhances yield in algal biofuel assemblages, *Journal of Applied Ecology*. 51 (2014) 603–611. <https://doi.org/10.1111/1365-2664.12242>.
- [34] D.N. Carruthers, C.K. Byun, B.J. Cardinale, X.N. Lin, Demonstration of transgressive overyielding of algal mixed cultures in microdroplets, *Integrative Biology*. 9 (2017) 687–694. <https://doi.org/10.1039/C6IB00241B>.
- [35] N. Renuka, A. Sood, S.K. Ratha, R. Prasanna, A.S. Ahluwalia, Evaluation of microalgal consortia for treatment of primary treated sewage effluent and biomass production, *J Appl Phycol*. 25 (2013) 1529–1537. <https://doi.org/10.1007/s10811-013-9982-x>.

- [36] S.P. Cuellar-Bermudez, G.S. Aleman-Nava, R. Chandra, J.S. Garcia-Perez, J.R. Contreras-Angulo, G. Markou, K. Muylaert, B.E. Rittmann, R. Parra-Saldivar, Nutrients utilization and contaminants removal. A review of two approaches of algae and cyanobacteria in wastewater, *Algal Research*. 24 (2017) 438–449. <https://doi.org/10.1016/j.algal.2016.08.018>.
- [37] J. Roostaei, Y. Zhang, Spatially Explicit Life Cycle Assessment: Opportunities and challenges of wastewater-based algal biofuels in the United States, *Algal Research*. 24 (2017) 395–402. <https://doi.org/10.1016/j.algal.2016.08.008>.
- [38] B.K. Shurtz, B. Wood, J.C. Quinn, Nutrient resource requirements for large-scale microalgae biofuel production: Multi-pathway evaluation, *Sustainable Energy Technologies and Assessments*. 19 (2017) 51–58. <https://doi.org/10.1016/j.seta.2016.11.003>.
- [39] Alternative Fuel Transportation Program; Replacement Fuel Goal Modification, *Federal Register*. (2007). <https://www.federalregister.gov/documents/2007/03/15/E7-4324/alternative-fuel-transportation-program-replacement-fuel-goal-modification> (accessed July 21, 2022).
- [40] M. Passero, B. Cragin, E.R. Coats, A.G. McDonald, K. Feris, Dairy Wastewaters for Algae Cultivation, Polyhydroxyalkanoate Reactor Effluent Versus Anaerobic Digester Effluent, *Bioenerg. Res.* 8 (2015) 1647–1660. <https://doi.org/10.1007/s12155-015-9619-9>.
- [41] O. US EPA, How Does Anaerobic Digestion Work?, (2019). <https://www.epa.gov/agstar/how-does-anaerobic-digestion-work> (accessed July 22, 2022).
- [42] E.R. Coats, E. Searcy, K. Feris, D. Shrestha, A.G. McDonald, A. Briones, T. Magnuson, M. Prior, An integrated two-stage anaerobic digestion and biofuel production process to reduce life cycle GHG emissions from US dairies, *Biofuels, Bioprod. Bioref.* 7 (2013) 459–473. <https://doi.org/10.1002/bbb.1408>.

- [43] O. US EPA, Anaerobic Digestion on Dairy Farms, (2021).  
<https://www.epa.gov/agstar/anaerobic-digestion-dairy-farms> (accessed July 22, 2022).
- [44] E.R. Coats, B.S. Watson, C.K. Brinkman, Polyhydroxyalkanoate synthesis by mixed microbial consortia cultured on fermented dairy manure: Effect of aeration on process rates/yields and the associated microbial ecology, *Water Research*. 106 (2016) 26–40. <https://doi.org/10.1016/j.watres.2016.09.039>.
- [45] A. Surendran, M. Lakshmanan, J.Y. Chee, A.M. Sulaiman, D.V. Thuoc, K. Sudesh, Can Polyhydroxyalkanoates Be Produced Efficiently From Waste Plant and Animal Oils?, *Frontiers in Bioengineering and Biotechnology*. 8 (2020).  
<https://www.frontiersin.org/articles/10.3389/fbioe.2020.00169> (accessed July 22, 2022).
- [46] O.S. Djandja, Z. Wang, L. Chen, L. Qin, F. Wang, Y. Xu, P. Duan, Progress in Hydrothermal Liquefaction of Algal Biomass and Hydrothermal Upgrading of the Subsequent Crude Bio-Oil: A Mini Review, *Energy Fuels*. 34 (2020) 11723–11751. <https://doi.org/10.1021/acs.energyfuels.0c01973>.
- [47] M. Bidy, R. Davis, S. Jones, Whole Algae Hydrothermal Liquefaction Technology Pathway, National Renewable Energy Lab. (NREL), Golden, CO (United States), 2013. <https://doi.org/10.2172/1076659>.
- [48] A.R.K. Gollakota, N. Kishore, S. Gu, A review on hydrothermal liquefaction of biomass, *Renewable and Sustainable Energy Reviews*. 81 (2018) 1378–1392.  
<https://doi.org/10.1016/j.rser.2017.05.178>.
- [49] U. Jena, K.C. Das, J.R. Kastner, Effect of operating conditions of thermochemical liquefaction on biocrude production from *Spirulina platensis*, *Bioresource Technology*. 102 (2011) 6221–6229.  
<https://doi.org/10.1016/j.biortech.2011.02.057>.

- [50] Y. Zhu, S.B. Jones, A.J. Schmidt, K.O. Albrecht, S.J. Edmundson, D.B. Anderson, Techno-economic analysis of alternative aqueous phase treatment methods for microalgae hydrothermal liquefaction and biocrude upgrading system, *Algal Research*. 39 (2019) 101467. <https://doi.org/10.1016/j.algal.2019.101467>.
- [51] S. Leow, J.R. Witter, D.R. Vardon, B.K. Sharma, J.S. Guest, T.J. Strathmann, Prediction of microalgae hydrothermal liquefaction products from feedstock biochemical composition, *Green Chem*. 17 (2015) 3584–3599. <https://doi.org/10.1039/C5GC00574D>.
- [52] P.-G. Duan, S.-K. Yang, Y.-P. Xu, F. Wang, D. Zhao, Y.-J. Weng, X.-L. Shi, Integration of hydrothermal liquefaction and supercritical water gasification for improvement of energy recovery from algal biomass, *Energy*. 155 (2018) 734–745. <https://doi.org/10.1016/j.energy.2018.05.044>.
- [53] P.H. Chen, J.L. Venegas Jimenez, S.M. Rowland, J.C. Quinn, L.M.L. Laurens, Nutrient recycle from algae hydrothermal liquefaction aqueous phase through a novel selective remediation approach, *Algal Research*. 46 (2020) 101776. <https://doi.org/10.1016/j.algal.2019.101776>.
- [54] N. Chernova, S. Kiseleva, M. Vlaskin, A. Grigorenko, Recycling of Aqueous Phase from Hydrothermal Liquefaction and Municipal Wastewater by Microalgae, *IOP Conf. Ser.: Mater. Sci. Eng.* 877 (2020) 012045. <https://doi.org/10.1088/1757-899X/877/1/012045>.
- [55] S.P. Singh, P. Singh, Effect of temperature and light on the growth of algae species: A review, *Renewable and Sustainable Energy Reviews*. 50 (2015) 431–444. <https://doi.org/10.1016/j.rser.2015.05.024>.
- [56] C. Largeau, E. Casadevall, C. Berkaloff, P. Dhamelin court, Sites of accumulation and composition of hydrocarbons in *Botryococcus braunii*, *Phytochemistry*. 19 (1980) 1043–1051. [https://doi.org/10.1016/0031-9422\(80\)83054-8](https://doi.org/10.1016/0031-9422(80)83054-8).



- [57] T. Masuko, A. Minami, N. Iwasaki, T. Majima, S.-I. Nishimura, Y.C. Lee, Carbohydrate analysis by a phenol–sulfuric acid method in microplate format, *Analytical Biochemistry*. 339 (2005) 69–72.  
<https://doi.org/10.1016/j.ab.2004.12.001>.
- [58] B. Cremella, Y. Huot, S. Bonilla, Interpretation of total phytoplankton and cyanobacteria fluorescence from cross-calibrated fluorometers, including sensitivity to turbidity and colored dissolved organic matter, *Limnology and Oceanography: Methods*. 16 (2018) 881–894.  
<https://doi.org/10.1002/lom3.10290>.
- [59] M. Kula, H.M. Kalaji, A. Skoczowski, Culture density influence on the photosynthetic efficiency of microalgae growing under different spectral compositions of light, *Journal of Photochemistry and Photobiology B: Biology*. 167 (2017) 290–298. <https://doi.org/10.1016/j.jphotobiol.2017.01.013>.
- [60] N. Saxena, Y. Chudasama, H. Chawada, S. Kodgire, S. Dasgupta, D. Sanyal, Evaluating Total Organic Carbon Derived Algae Biomass Productivity Compared with Ash Free Dry Weight Measurement, *Proc. Natl. Acad. Sci., India, Sect. B Biol. Sci.* 91 (2021) 89–94. <https://doi.org/10.1007/s40011-020-01200-3>.
- [61] J.M. Ayre, N.R. Moheimani, M.A. Borowitzka, Growth of microalgae on undiluted anaerobic digestate of piggery effluent with high ammonium concentrations, *Algal Research*. 24 (2017) 218–226.  
<https://doi.org/10.1016/j.algal.2017.03.023>.
- [62] S. Feng, F. Liu, S. Zhu, P. Feng, Z. Wang, Z. Yuan, C. Shang, H. Chen, Performance of a microalgal-bacterial consortium system for the treatment of dairy-derived liquid digestate and biomass production, *Bioresource Technology*. 306 (2020) 123101. <https://doi.org/10.1016/j.biortech.2020.123101>.
- [63] W. Yang, Z. Wang, J. Han, S. Song, Y. Zhang, W. Gong, The role of polysaccharides and proteins in bio-oil production during the hydrothermal liquefaction of algae species, *RSC Adv.* 9 (n.d.) 41962–41969.  
<https://doi.org/10.1039/c9ra07150d>.

- [64] M.A. Yaakob, R.M.S.R. Mohamed, A. Al-Gheethi, R. Aswathnarayana Gokare, R.R. Ambati, Influence of Nitrogen and Phosphorus on Microalgal Growth, Biomass, Lipid, and Fatty Acid Production: An Overview, *Cells*. 10 (2021) 393. <https://doi.org/10.3390/cells10020393>.
- [65] F. Bélanger-Lépine, A. Tremblay, Y. Huot, S. Barnabé, Cultivation of an algae-bacteria consortium in wastewater from an industrial park: Effect of environmental stress and nutrient deficiency on lipid production, *Bioresource Technology*. 267 (2018) 657–665. <https://doi.org/10.1016/j.biortech.2018.07.099>.
- [66] W. Michelon, M.L.B. Da Silva, M.P. Mezzari, M. Pirolli, J.M. Prandini, H.M. Soares, Effects of Nitrogen and Phosphorus on Biochemical Composition of Microalgae Polyculture Harvested from Phycoremediation of Piggery Wastewater Digestate, *Appl Biochem Biotechnol*. 178 (2016) 1407–1419. <https://doi.org/10.1007/s12010-015-1955-x>.
- [67] S. Deshmukh, R. Kumar, K. Bala, Microalgae biodiesel: A review on oil extraction, fatty acid composition, properties and effect on engine performance and emissions, *Fuel Processing Technology*. 191 (2019) 232–247. <https://doi.org/10.1016/j.fuproc.2019.03.013>.
- [68] L. Qin, Z. Wang, Y. Sun, Q. Shu, P. Feng, L. Zhu, J. Xu, Z. Yuan, Microalgae consortia cultivation in dairy wastewater to improve the potential of nutrient removal and biodiesel feedstock production, *Environ Sci Pollut Res*. 23 (2016) 8379–8387. <https://doi.org/10.1007/s11356-015-6004-3>.
- [69] E. Monfet, A. Unc, Defining wastewaters used for cultivation of algae, *Algal Research*. 24 (2017) 520–526. <https://doi.org/10.1016/j.algal.2016.12.008>.
- [70] A.M. Rada-Ariza, D. Fredy, C.M. Lopez-Vazquez, N.P. Van der Steen, P.N.L. Lens, Ammonium removal mechanisms in a microalgal-bacterial sequencing-batch photobioreactor at different solids retention times, *Algal Research*. 39 (2019) 101468. <https://doi.org/10.1016/j.algal.2019.101468>.

- [71] Q. Wang, J. Cheronos, B. Higgins, Acclimation of an algal consortium to sequester nutrients from anaerobic digestate, *Bioresource Technology*. 342 (2021) 125921. <https://doi.org/10.1016/j.biortech.2021.125921>.
- [72] J. Wang, W. Zhou, H. Chen, J. Zhan, C. He, Q. Wang, Ammonium Nitrogen Tolerant *Chlorella* Strain Screening and Its Damaging Effects on Photosynthesis, *Frontiers in Microbiology*. 9 (2019). <https://www.frontiersin.org/articles/10.3389/fmicb.2018.03250> (accessed July 26, 2022).
- [73] Y. Zhou, L. Schideman, G. Yu, Y. Zhang, A synergistic combination of algal wastewater treatment and hydrothermal biofuel production maximized by nutrient and carbon recycling, *Energy & Environmental Science*. 6 (2013) 3765–3779. <https://doi.org/10.1039/C3EE24241B>.
- [74] Z. Li, L. Haifeng, Y. Zhang, M. Shanshan, L. Baoming, L. Zhidan, D. Na, L. Minsheng, S. Buchun, L. Jianwen, Effects of strain, nutrients concentration and inoculum size on microalgae culture for bioenergy from post hydrothermal liquefaction wastewater, *International Journal of Agricultural and Biological Engineering*. 10 (2017) 194–204. <https://doi.org/10.25165/ijabe.v10i2.2882>.
- [75] R. Pate, G. Klise, B. Wu, Resource demand implications for US algae biofuels production scale-up, *Applied Energy*. 88 (2011) 3377–3388. <https://doi.org/10.1016/j.apenergy.2011.04.023>.
- [76] Z. Li, Y. Zhou, H. Yang, D. Zhang, C. Wang, H. Liu, X. Li, J. Zhao, C. Wei, A novel strategy and kinetics analysis of half-fractional high cell density fed-batch cultivation of *Zygosaccharomyces rouxii*, *Food Sci Nutr*. 6 (2018) 1162–1169. <https://doi.org/10.1002/fsn3.666>.
- [77] O. US EPA, Water Quality Trading, (2016). <https://www.epa.gov/npdes/water-quality-trading> (accessed July 30, 2022).
- [78] T. Wade, T. Borisova, Water Quality Credit Trading: General Principles, General Principles. (2022) 8.

- [79] J.M. Duke, H. Liu, T. Monteith, J. McGrath, N.M. Fiorellino, A method for predicting participation in a performance-based water quality trading program, *Ecological Economics*. 177 (2020) 106762.  
<https://doi.org/10.1016/j.ecolecon.2020.106762>.
- [80] A.C. Redfield, *On the Proportions of Organic Derivatives in Sea Water and Their Relation to the Composition of Plankton*, University Press of Liverpool, 1934.
- [81] Current&nbsp;West Texas Intermediate Crude Oil (WTI) Prices, (n.d.).  
<http://www.up.com/up/customers/surcharge/wti/prices/index.htm> (accessed July 31, 2022).
- [82] M. Langemeier, Explaining Fluctuations in DDG Prices, *Farmdoc Daily*. 12 (2022). <https://farmdocdaily.illinois.edu/2022/06/explaining-fluctuations-in-ddg-prices-2.html> (accessed July 31, 2022).